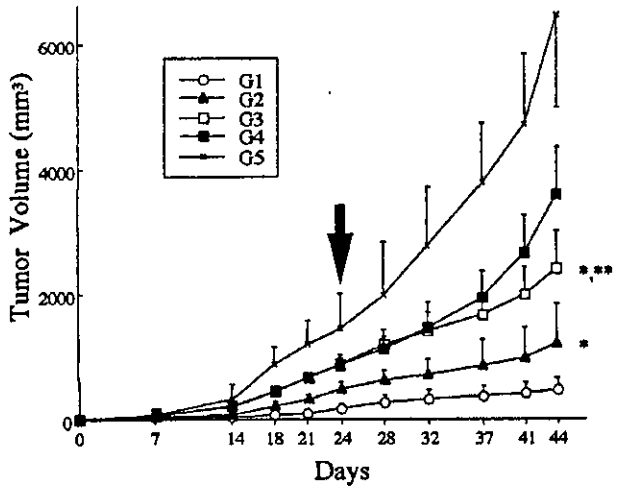

Fig. 3. Effect of bFGF and VEGF expression on BNL-HCC growth. Tet-bFGF-transduced clone (bFGF-HCC), Tet-VEGF- and Pcl-VEGF-transduced clone (bFGF-VEGF-HCC), and Tet-*lacZ*-transduced clone (*lacZ*-HCC) were injected subcutaneously into BALB/c mice. G1 consisted of *lacZ*-HCC-injected mice and served as a control. The animals in G2 were injected with bFGF-HCC cells and drank tet-free normal water to maintain bFGF overexpression throughout the experiment (bFGF [+]: G2). The G3 and G4 animals were bFGF-VEGF-HCC-transplanted groups. Both groups first drank tet-containing water. The animals in G3 received tet-containing water throughout the experiment to suppress bFGF expression under the constitutive VEGF overexpression (VEGF [+]: G3). The water given to the animals in G4 was changed from tet-containing to normal water on day 28 (mean tumor volume was 1,426 mm³) to switch on bFGF expression in addition to VEGF overexpression (VEGF [+] + bFGF [− > +]: G4). The mice in G5 also received transplanted bFGF-VEGF-HCC cells and drank tet-free water until the end of experiment to maintain both overexpression of bFGF and VEGF (VEGF [+] + bFGF [+]). Expression of bFGF was controlled by tet (tet: 1 mg/mL) in the drinking water. Each group consisted of 10 animals. The **arrow** indicates the time point at which tet was removed from the drinking water in G4. The tumor volume was determined by caliper at the indicated time points. Each point represents the mean ± SD of 16 animals. *, **Statistically significant differences compared with G1 and G2, respectively ($P < .01$).

Effect of bFGF and VEGF on Subcutaneous Tumor Growth. To examine the effect of bFGF and VEGF on tumor development *in vivo*, bFGF-HCC and bFGF-VEGF-HCC cells were injected into the flank of BALB/c mice. When compared with the *lacZ*-HCC control group (G1), both bFGF (G2) and VEGF (G3) overexpression revealed a marked increase in tumor development ($P < .01$). The magnitude of augmentation was stronger in G3 than G2 ($P < .01$). The combined expression of bFGF and VEGF (G5) revealed a drastically increased level of tumor development, and this tumor growth increase effect was much more than the additive effect of the bFGF (G2) and VEGF (G3) groups. We next examined the effect of bFGF modulation after the tumor was established. In G4, bFGF expression changed to the on state from day 28 as a result of drinking normal water from tet-containing water, under the condition of constitutive VEGF overexpression. After bFGF overexpression, the tumor growth rate in G4 became much faster than G3. This tumor growth augmentation also seemed to exceed the additive effect of bFGF, and the growth curve was similar to that of G5 (Fig. 3). VEGF and bFGF expression in the tumors were maintained at a similar level to those of the cells *in vitro*, and tet did not affect the healthy state, such as body weight during the experiment (data not shown).

***Tumor Neovascularization* In Vivo.** To determine whether the increased tumor growth rate was associated with bFGF- and VEGF-induced neovascularization, we examined the tumor expression level of CD 31, which is widely used as a marker of neovascularization. We found that bFGF and VEGF overexpression led a significant increase in CD31-immunopositive vessels of the tumor (Fig. 4). The magnitude of CD31-positive vessel augmentation was likely to correspond to the tumor development. Because it has been shown recently that image analysis was more reliable and objective than manual counts of microvessels, we employed computer-assisted image analysis techniques as described previously.[46] A semiquantitative analysis of CD31-positive vessels revealed that neovascularization in the tumors consisting of bFGF-HCC, VEGF-HCC, and bFGF-VEGF-HCC cells showed 1.66-, 3.42-, and 8.15-fold increases compared with the control group, respectively (Fig. 5).

Role of VEGF and KDR/Flk-1 in bFGF-Induced Tumor Growth. To elucidate the possible interaction of bFGF and VEGF, we examined the effect of KDR/Flk-1 mAb on bFGF-induced tumor growth *in vivo*. As described above, bFGF-HCC cells showed a significant increase in tumor development compared with the *lacZ*-HCC control group ($P < .01$). When bFGF was suppressed in the tumor by the addition of tet to drinking water, tumor growth was decreased a similar level as the control group. This indicates that the bFGF-induced tumor growth kinetics in this study could be attributed exclusively to bFGF expression. As shown in Table 1, real-time PCR revealed that VEGF messenger RNA (mRNA) expression was 3.1-fold higher in the bFGF-overexpressed tumor than the bFGF-suppressed tumor. Furthermore, we found that bFGF-induced tumor

Table 1. Effect of bFGF on VEGF Gene Expression In Animals With Tet-bFGF Tumors

	bFGF (−)	bFGF (+)
VEGF gene expression	1.42 ± 0.36*	4.40 ± 1.22

NOTE. bFGF (−) and (+) denote bFGF suppression and overexpression in the tumor by tetracycline (1 mg/mL) of the drinking water, respectively ($n = 5$).

*Gene expression presented after normalization with the glyceraldehyde-3-phosphate dehydrogenase internal control.

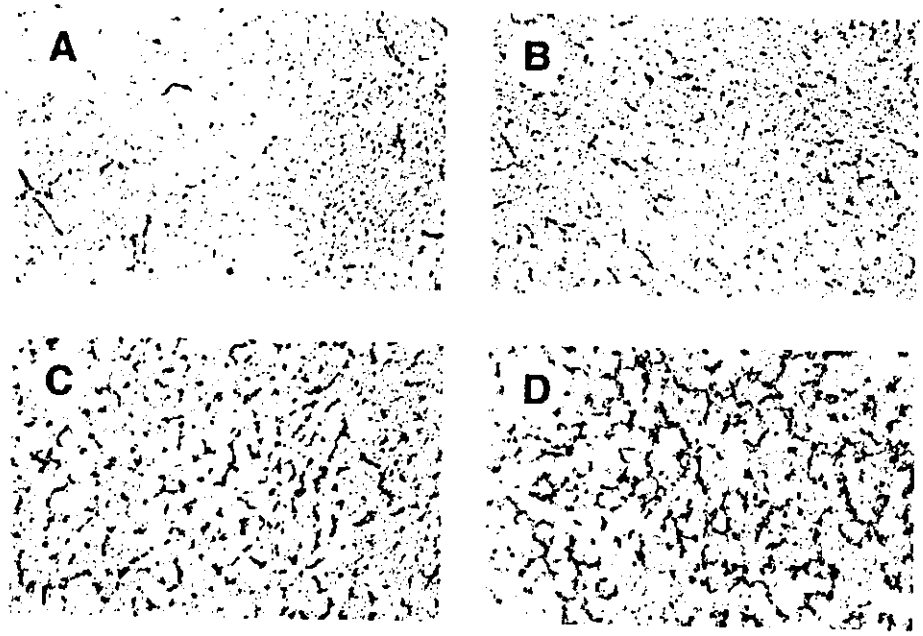

Fig. 4. Effect of bFGF and VEGF on CD31 expression in the tumors. Tumor vasculaturization was visualized by immunostaining of CD31 vascular endothelial adhesion protein. (A) *LacZ*-transduced control group (G1). (B) bFGF-HCC group (G2). (C) VEGF-HCC group (G3). (D) bFGF-VEGF-HCC group (G5). The description of each group is shown in the Materials and Methods section. Original magnification ×200.

growth augmentation was significantly suppressed by KDR/Flk-1 mAb treatment ($P < .01$) (Fig. 6). In the bFGF-suppressed tumor, KDR/Flk-1 mAb treatment did not show any significant effect on the tumor growth (data not shown). These results suggested that VEGF is an important downstream mediator of bFGF-induced tumor development, and this VEGF-mediated effect was achieved mostly through KDR/Flk-1.

Discussion

Emerging evidence has shown that tumor growth beyond a few millimeters is dependent on the induction of angiogenesis mediated by the release of angiogenic factors secreted by the tumor cells. Tumors secrete a wide variety of angiogenic factors that participate in the development of microvasculature in the tumor.[1-5] It is been recognized that *in vivo* angiogenesis status is determined by a balance of several regulators, rather than by a single regulator alone. The angiogenic activity of a cytokine such as VEGF is contextual, because it depends on interactions with other factors present in the endothelial pericellular environment.[6-8] Among the identified angiogenic factors, VEGF and bFGF are the most potent and representative angiogenic factors.[6-11]

HCC is recognized to be a distinctively hypervascular tumor in clinical practice. Several reports have been shown that VEGF and bFGF were highly expressed in human HCC.[13,15,17,36-38] Most of reports showed that VEGF expression was increased in HCC regions than noncancerous tissues.[13,15,17] In animal studies, we have shown that VEGF played a pivotal role of HCC development, and its biologic effect was mainly mediated by KDR/Flk-1.[1-5,39,40] Although expression of bFGF was discovered in HCC cells, no substantial correlation was observed with clinicopathologic parameters. It has been suggested that VEGF contributed to angiogenesis of HCC, whereas bFGF may be involved in the invasion of HCC into the surrounding tissues.[13] VEGF, originally identified as a vascular permeability factor, is the most

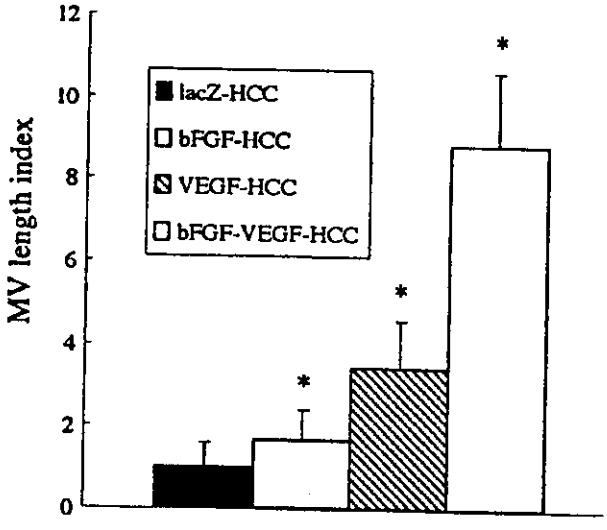

Fig. 5. Semiquantitative analysis of CD31-immunopositive vessels. The length of immunopositive vessels in the tumor were measured by an image analysis system. The description of each group is shown in the Materials and Methods section. The data represent the mean ± SD ($n = 5$). *A statistically significant difference compared with the *lacZ*-HCC control group ($P < .01$). MV, microvessel.

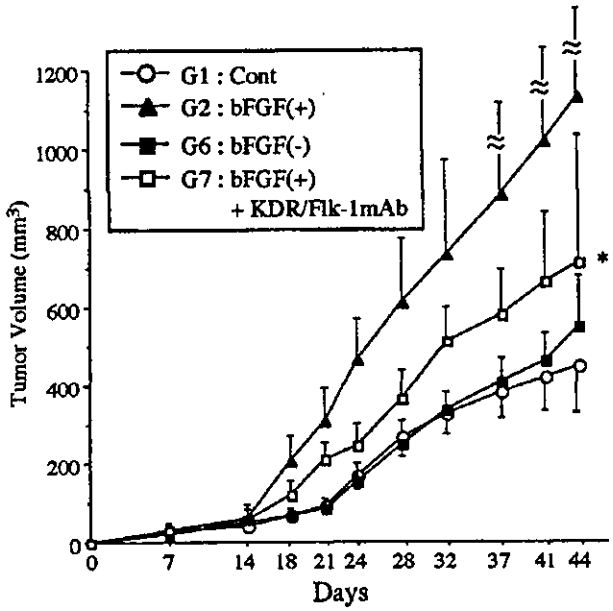

Fig. 6. The growth effect of KDR/Flk-1 mAb-mediated suppression of bFGF-induced tumor development. G1 is the *lac-z*-HCC control group. The mice in G2, G6 and G7 received transplanted bFGF-HCC cells. To maintain bFGF overexpression or suppression, mice in G2 (bFGF [+]), G7 were given tet-free normal water and G6 (bFGF [−]) was given tet-containing drinking water throughout the experiment, respectively. The animals in G7 were injected with KDR/Flk-1 mAb (bFGF [+] + KDR/Flk-1 mAb), and all other groups were injected with same amount of the control immunoglobulin G described as in the Materials and Methods section. The tumor volume was determined by caliper at the indicated time points. Each point represents the mean ± SD of 16 animals. *A statistically significant difference compared with G2 ($P < .01$).

intriguing factor in regard to tumor angiogenesis. Besides an angiogenic factor, VEGF also is known as a survival factor of newly formed EC.[49] In contrast to bFGF, VEGF has a typical signal peptide sequence and acts almost exclusively on EC.[6-8] In animal models, VEGF overexpression has been shown to enhance tumor growth, whereas suppression of VEGF inhibited tumor growth and angiogenesis.[1-5,29,30] To date, several reports have shown that either VEGF or bFGF single-gene manipulation altered tumor biologic behavior, such as tumor growth or angiogenesis.[12,29-33,39] The direct combination effect of bFGF and VEGF overexpression in tumor development and angiogenesis including HCC has not been elucidated yet.

In this study, we found that bFGF and VEGF showed a significant synergistic effect of HCC development and angiogenesis. Although both bFGF and VEGF increased HCC development and angiogenesis, the combined effect was much stronger than the additive effect of each factor. VEGF and bFGF have been reported to exert a synergistic effect on *in vitro* EC tubular formation and proliferation[21-27] and on *in vivo* hind limb ischemia or cornea angiogenesis assay.[22,28] Regarding the interaction between these molecules, bFGF has been shown to induce VEGF gene expression in EC, and VEGF neutralizing monoclonal antibody or VEGF antisense oligonucleotide treatment inhibited bFGF-induced EC proliferation *in vitro*.[22,27] In this study, we found that VEGF mRNA expression in the tumor was markedly increased by bFGF overexpression and that bFGF-induced tumor growth augmentation was inhibited by KDR/Flk-1 mAb. On the other hand, we did not find bFGF up-regulation by VEGF in BNL-HCC cells *in vitro* (data not shown). It is possible that the tumor environmental cells other than cancer cells such as EC were responsible for VEGF induction by bFGF as described previously.[21-28] Nevertheless, we cannot rule out the possibility that bFGF overexpression may affect biologic properties other than VEGF with possible consequences on VEGF induction in the tumor. Recently, it has been shown that conditional down-regulation of bFGF caused a significant decrease in tumor growth and angiogenesis in the endometrial adenocarcinoma cells.[31] In contrast to our present study, the authors found that intratumoral VEGF level was not affected by bFGF expression. The reason for this discrepancy remains obscure; however, it is possible that bFGF and VEGF may exert tumor cell type–specific biologic interaction behavior. The *in vivo* interactions of both factors described here merit further investigations.

In summary, the present study revealed that bFGF and VEGF showed a synergistic effect on HCC development and angiogenesis by combination of Retro-Tet and the conventional gene expression system. The VEGF mRNA expression was increased by bFGF overexpression in the tumor, and bFGF-induced tumor augmentation was significantly suppressed by KDR/Flk-1 mAb. These results suggest that VEGF is located downstream of bFGF-induced HCC development, and the VEGF-mediated effect occurs mostly through KDR/Flk-1.

References

1. Carmeliet P, Jain RK. Angiogenesis in cancer and other diseases. Nature 2000;407:249-257.
2. Kerbel RS. Tumor angiogenesis: past, present and the near future. Carcinogenesis 2000;21:505-515.
3. Folkman J. Angiogenesis in cancer, vascular, rheumatoid and other disease. Nat Med 1995;1:27-31.
4. Fox SB, Gatter KC, Harris AL. Tumour angiogenesis. J Pathol 1996;179:232-237.
5. Fidler IJ, Ellis LM. The implications of angiogenesis for the biology and therapy of cancer metastasis. Cell 1994;79:185-188.
6. Shibuya M. Role of VEGF-flt receptor system in normal and tumor angiogenesis. Adv Cancer Res 1995;67:281-316.
7. Dvorak HF, Brown LF, Detmar M, Dvorak AM. Vascular permeability factor/vascular endothelial growth factor, microvascular hyperpermeability, and angiogenesis. Am J Pathol 1995;146:1029-1039.

8. Karkkainen MJ, Petrova TV. Vascular endothelial growth factor receptors in the regulation of angiogenesis and lymphangiogenesis. Oncogene 2000;19:5598-5605.
9. Nugent MA, Iozzo RV. Fibroblast growth factor-2. Int J Biochem Cell Biol 2000;32:115-120.
10. Gospodarowicz D. Fibroblast growth factor. Chemical structure and biologic function. Clin Orthop 1990;231-248.
11. Gospodarowicz D, Neufeld G, Schweigerer L. Fibroblast growth factor: structural and biological properties. J Cell Physiol Suppl 1987;(Suppl)15-26.
12. Kandel J, Bossy-Wetzel E, Radvanyi F, Klagsbrun M, Folkman J, Hanahan D. Neovascularization is associated with a switch to the export of bFGF in the multistep development of fibrosarcoma. Cell 1991;66:1095-1104.
13. Mise M, Arii S, Higashituji H, Furutani M, Niwano M, Harada T, Ishigami S, et al. Clinical significance of vascular endothelial growth factor and basic fibroblast growth factor gene expression in liver tumor. HEPATOLOGY 1996;23:455-464.
14. Samoto K, Ikezaki K, Ono M, Shono T, Kohno K, Kuwano M, Fukui M. Expression of vascular endothelial growth factor and its possible relation with neovascularization in human brain tumors. Cancer Res 1995;55:1189-1193.
15. Suzuki K, Hayashi N, Miyamoto Y, Yamamoto M, Ohkawa K, Ito Y, Sasaki Y, et al. Expression of vascular permeability factor/vascular endothelial growth factor in human hepatocellular carcinoma. Cancer Res 1996;56:3004-3009.
16. Yoshiji H, Gomez DE, Shibuya M, Thorgeirsson UP. Expression of vascular endothelial growth factor, its receptor, and other angiogenic factors in human breast cancer. Cancer Res 1996;56: 2013-2016.
17. Yamaguchi R, Yano H, Iemura A, Ogasawara S, Haramaki M, Kojiro M. Expression of vascular endothelial growth factor in human hepatocellular carcinoma. HEPATOLOGY 1998;28:68-77.
18. Waltenberger J, Claesson-Welsh L, Siegbahn A, Shibuya M, Heldin CH. Different signal transduction properties of KDR and Flt1, two receptors for vascular endothelial growth factor. J Biol Chem 1994;269:26988-26995.
19. Kroll J, Waltenberger J. The vascular endothelial growth factor receptor KDR activates multiple signal transduction pathways in porcine aortic endothelial cells. J Biol Chem 1997;272:32521-32527.
20. Millauer B, Longhi MP, Plate KH, Shawver LK, Risau W, Ullrich A, Strawn LM. Dominant-negative inhibition of Flk-1 suppresses the growth of many tumor types in vivo. Cancer Res 1996;56: 1615-1620.
21. Goto F, Goto K, Weindel K, Folkman J. Synergistic effects of vascular endothelial growth factor and basic fibroblast growth factor on the proliferation and cord formation of bovine capillary endothelial cells within collagen gels. Lab Invest 1993;69:508-517.
22. Seghezzi G, Patel S, Ren CJ, Gualandris A, Pintucci G, Robbins ES, Shapiro RL, et al. Fibroblast growth factor-2 (FGF-2) induces vascular endothelial growth factor (VEGF) expression in the endothelial cells of forming capillaries: an autocrine mechanism contributing to angiogenesis. J Cell Biol 1998;141: 1659-1673.
23. Mandriota SJ, Pepper MS. Vascular endothelial growth factor-induced in vitro angiogenesis and plasminogen activator expression are dependent on endogenous basic fibroblast growth factor. J Cell Sci 1997;110:2293-2302.
24. Hata Y, Rook SL, Aiello LP. Basic fibroblast growth factor induces expression of VEGF receptor KDR through a protein kinase C and p44/p42 mitogen-activated protein kinase–dependent pathway. Diabetes 1999;48:1145-1155.
25. Tokuda H, Kozawa O, Uematsu T. Basic fibroblast growth factor stimulates vascular endothelial growth factor release in osteoblasts: divergent regulation by p42/p44 mitogen-activated protein kinase and p38 mitogen-activated protein kinase. J Bone Miner Res 2000;15:2371-2379.
26. Saadeh PB, Mehrara BJ, Steinbrech DS, Spector JA, Greenwald JA, Chin GS, Ueno H, et al. Mechanisms of fibroblast growth factor-2 modulation of vascular endothelial growth factor expression by osteoblastic cells. Endocrinology 2000;141: 2075-2083.
27. Majima M, Hayashi I, Muramatsu M, Katada J, Yamashina S, Katori M. Cyclo-oxygenase-2 enhances basic fibroblast growth factor-induced angiogenesis through induction of vascular endothelial growth factor in rat sponge implants. Br J Pharmacol 2000; 130:641-649.
28. Asahara T, Bauters C, Zheng LP, Takeshita S, Bunting S, Ferrara N, Symes JF, et al. Synergistic effect of vascular endothelial growth factor and basic fibroblast growth factor on angiogenesis in vivo. Circulation 1995;92:II365-II371.
29. Cheng SY, Huang HJ, Nagane M, Ji XD, Wang D, Shih CC, Arap W, et al. Suppression of glioblastoma angiogenicity and tumorigenicity by inhibition of endogenous expression of vascular endothelial growth factor. Proc Natl Acad Sci U S A 1996;93: 8502-8507.
30. Yoshiji H, Harris SR, Thorgeirsson UP. Vascular endothelial growth factor is essential for initial but not continued in vivo growth of human breast carcinoma cells. Cancer Res 1997;57: 3924-3928.
31. Giavazzi R, Giuliani R, Coltrini D, Bani MR, Ferri C, Sennino B, Tosatti MPM, et al. Modulation of tumor angiogenesis by conditional expression of fibroblast growth factor-2 affects early but not established tumors. Cancer Res 2001;61:309-317.
32. Coltrini D, Gualandris A, Nelli EE, Parolini S, Molinari-Tosatti MP, Quarto N, Ziche M, et al. Growth advantage and vascularization induced by basic fibroblast growth factor overexpression in endometrial HEC-1-B cells: an export-dependent mechanism of action. Cancer Res 1995;55:4729-4738.
33. Wang Y, Becker D. Antisense targeting of basic fibroblast growth factor and fibroblast growth factor receptor-1 in human melanomas blocks intratumoral angiogenesis and tumor growth. Nat Med 1997;3:887-893.
34. Simonetti RG, Camma C, Fiorello F, Politi F, D'Amico G, Pagliaro L. Hepatocellular carcinoma. A worldwide problem and the major risk factors. Dig Dis Sci 1991;36:962-972.
35. Hatori N. Epidemiology of liver cancer in Japan. J Clin Exp Med 1994;171:1097-1104.
36. Ogasawara S, Yano H, Iemura A, Hisaka T, Kojiro M. Expressions of basic fibroblast growth factor and its receptors and their relationship to proliferation of human hepatocellular carcinoma cell lines. HEPATOLOGY 1996;24:198-205.
37. Kin M, Sata M, Ueno T, Torimura T, Inuzuka S, Tsuji R, Sujaku K, et al. Basic fibroblast growth factor regulates proliferation and motility of human hepatoma cells by an autocrine mechanism. J Hepatol 1997;27:677-687.
38. Chow NH, Cheng KS, Lin PW, Chan SH, Su WC, Sun YN, Lin XZ. Expression of fibroblast growth factor-1 and fibroblast

growth factor-2 in normal liver and hepatocellular carcinoma. Dig Dis Sci 1998;43:2261-2266.
39. Yoshiji H, Kuriyama S, Yoshii J, Yamazaki M, Kikukawa M, Tsujinoue H, Nakatani T, et al. Vascular endothelial growth factor tightly regulates in vivo development of murine hepatocellular carcinoma cells. HEPATOLOGY 1998;28:1489-1496.
40. Yoshiji H, Kuriyama S, Hicklin DJ, Huber J, Yoshii J, Miyamoto Y, Kawata M, et al. KDR/Flk-1 is a major regulator of vascular endothelial growth factor–induced tumor development and angiogenesis in murine hepatocellular carcinoma cells. HEPATOLOGY 1999;30:1179-1186.
41. Gossen M, Bujard H. Tight control of gene expression in mammalian cells by tetracycline-responsive promoters. Proc Natl Acad Sci U S A 1992;89:5547-5551.
42. Gately S, Tsanaclis AM, Takano S, Klagsbrun M, Brem S. Cells transfected with the basic fibroblast growth factor gene fused to a signal sequence are invasive in vitro and in situ in the brain. Neurosurgery 1995;36:780-788.
43. Einar K, Halsor EF. Vascular endothelial growth factor, interleukin 8, platelet-derived endothelial cell growth factor, and basic fibroblast growth factor promote angiogenesis and metastasis in human melanoma xenografts. Cancer Res 2000;60:4932-4938.
44. Yoshiji H, Kuriyama S, Ways DK, Yoshii J, Miyamoto Y, Kawata M, Ikenaka Y, et al. Protein kinase C lies on the signaling pathway for vascular endothelial growth factor-mediated tumor development and angiogenesis. Cancer Res 1999;59:4413-4418.
45. Yoshiji H, Kuriyama S, Kawata M, Yoshii J, Ikenaka Y, Noguchi R, Nakatani T, et al. The angiotensin-I converting enzyme inhibitor, perindopril, suppresses tumor growth and angiogenesis: possible role of the vascular endothelial growth factor. Clin Cancer Res 2001;7:1073-1078.
46. Tanigawa N, Lu C, Mitsui T, Miura S. Quantitation of sinusoid-like vessels in hepatocellular carcinoma: its clinical and prognostic significance. HEPATOLOGY 1997;26:1216-1223.
47. Yoshiji H, Kuriyama S, Yoshii J, Ikenaka Y, Noguchi R, Nakatani T, Tsujinoue H, et al. Angiotensin-II type 1 receptor interaction is a major regulator for liver fibrosis development in rats. HEPATOLOGY 2001;34:745-750.
48. Gautschi O, Tschopp S, Olie RA, Leech SH, Simoes-Wust AP, Ziegler A, Baumann B, et al. Activity of a novel bcl-2/bcl-xL-bispecific antisense oligonucleotide against tumors of diverse histologic origins. J Natl Cancer Inst 2001;93:463-471.
49. Bruns CJ, Liu W, Davis DW, Shaheen RM, McConkey DJ, Wilson MR, Bucana CD, et al. Vascular endothelial growth factor is an in vivo survival factor for tumor endothelium in a murine model of colorectal carcinoma liver metastases. Cancer 2000;89:488-499.

ELSEVIER

Journal of Hepatology 37 (2002) 22–30

Journal of Hepatology

www.elsevier.com/locate/jhep

Inhibition of renin–angiotensin system attenuates liver enzyme-altered preneoplastic lesions and fibrosis development in rats

Hitoshi Yoshiji[1,*], Junichi Yoshii[1], Yasuhide Ikenaka[1], Ryuichi Noguchi[1], Hirohisa Tsujinoue[1], Toshiya Nakatani[1], Hiroo Imazu[1], Koji Yanase[1], Shigeki Kuriyama[2], Hiroshi Fukui[1]

[1]*Third Department of Internal Medicine, Nara Medical University, Shijo-cho 840, Kashihara, Nara 634-8522, Japan*
[2]*Third Department of Internal Medicine, Kagawa Medical University, Kagawa, Japan*

***Background/Aims*: It is suggested that the renin–angiotensin system (RAS) is involved in tumor development and fibrogenesis. The aim of the present study was to examine the effect of RAS inhibition on the liver enzyme-altered preneoplastic lesions and fibrosis development.**

***Methods*: The effects of the clinically used angiotensin-I converting enzyme inhibitor (ACE-I), perindopril (PE), on two different rat model of liver carcinogenesis models induced separately by diethylnitrosamine (DEN) and a choline-deficient L-amino acid-defined (CDAA) diet were studied. This CDAA model was also used to elucidate the effect of PE on liver fibrosis development.**

***Results*: The immunohistochemical evaluation revealed that the glutathione *S*-transferase placental form (GST-P), and γ-glutamyltransferase (GGT)-positive preneoplastic foci significantly decreased in the livers of the PE-treated groups. In CDAA-induced liver fibrosis model, PE revealed a marked inhibitory effect of liver fibrosis development. The hepatic hydroxyproline, serum fibrosis markers, α-smooth muscle actin (α-SMA) immunopositive cells in number, and α-(III) pro-collagen mRNA expression were significantly suppressed by PE treatment. These inhibitory effects of PE were achieved even at a clinically comparable dose (2 mg/kg per day).**

***Conclusions*: These results suggested that the RAS is involved in liver carcinogenesis and fibrosis development.**

***Keywords*: Renin–angiotensin system, Angiotensin-II, Angiotensin converting enzyme inhibitor, Hepatocarcinogenesis, Liver fibrosis**

1. Introduction

The renin–angiotensin system (RAS) is a key mediator in the regulation of arterial blood pressure and body fluid homeostasis [1,2]. The RAS also plays an important role in the regulation of local hemodynamics in several organs. In the liver, it has been shown that the RAS is frequently activated in the patients with chronic liver disease, such as cirrhosis [3–5]. Angiotensin-II (AT-II) is considered a potential mediator of portal hypertension, since its plasma level was significantly increased in patients with liver cirrhosis, and its administration induced elevation of the portal pressure [6,7]. AT-II has also been shown to induce contraction and proliferation of hepatic stellate cells (HSC), which play a pivotal role in liver fibrosis development [8,9]. Accordingly, it has been suggested that AT-II plays a role in liver fibrosis development.

In addition to fibrosis development, AT-II has been shown to induce neovascularization in experimental models both in vitro and in vivo [10–12], and it also selectively increased the blood flow in the tumor [13]. Angiogenesis is now widely recognized as playing a pivotal role in tumor development, including hepatocellular carcinoma (HCC) [14–16]. One of the characteristic features of HCC in clinical practice is a hypervascular tumor. In fact, several angiogenic factors significantly up-regulated in human HCC samples compared with the non-cancerous legions [17,18]. AT-II induces angiogenesis in several types of cells, including HCC, and activity of serum angiotensin-I converting

Received 4 October 2001; received in revised form 21 February 2002; accepted 22 March 2002

* Corresponding author. Tel.: +81-744-22-3051x3415; fax: +81-744-24-7122.

E-mail address: yoshijih@naramed-u.ac.jp (H. Yoshiji).

0168-8278/02/$20.00
PII: S0168-8278(02)00104-6

enzyme (ACE) was a tumor marker of HCC patients [12,19,20]. We previously reported that the clinically used ACE inhibitor (ACE-I), perindopril (PE) possesses a strong anti-angiogenic activity, and it inhibited the murine HCC growth [19]. Not only in established tumor growth, it is suggested that angiogenesis is now also involved in the early carcinogenesis step in several types of tumor [21–23]. In the liver, it has been revealed that angiogenesis was already markedly increased even at the stage of chronic hepatitis in hepatitis C-virus positive patients [24]. The role of AT-II, however, in liver carcinogenesis has not yet been elucidated.

The present study was conducted to examine the effect of RAS inhibition using the ACE-I, PE, on the liver preneoplastic foci and liver fibrosis development. We employed two different hepatocarcinogenesis models, one induced by the carcinogen, diethylnitrosamine (DEN model) [25–27], and the other induced by feeding on a choline-deficient, L-amino acid-defined diet without any carcinogen (CDAA model) [28–31]. The CDAA model exhibits pathological sequences similar to that of the human liver disease; namely hepatocellular necrosis, fibrotic change, cirrhosis, and finally HCC development [28–31]. Recently, it has been reported that the inhibition of RAS attenuated the experimental liver fibrosis development [32–34]. The effect of RAS inhibition, however, on CDAA-induced liver fibrosis development has not yet been elucidated. In the CDAA model, we examined the effect of PE on liver fibrosis and preneoplastic foci development.

2. Materials and methods

2.1. Animals

A total of 92 Male Fisher 344 rats, aged 6 weeks, were purchased from Japan SLC Inc. (Hamamatsu, Shizuoka, Japan). They were housed in stainless-steel mesh cages under control conditions of temperature (23 ± 3 °C) and relative humidity (50 ± 20%), with 10–15 air changes per hour and light illumination for 12 h a day. The animals were allowed access to food and tap water ad libitum throughout the acclimatization and experimental periods.

2.2. Compound and diets

The ACE-I, perindopril (PE) and a herbal medicine, Sho-saiko-to (TJ-9) were supplied from Daiichi Pharmaceutical Co. (Tokyo, Japan) and Tsumura (Tokyo, Japan), respectively. TJ-9 has been shown to prevent liver fibrosis, preneoplastic foci, and HCC development [35–37]. DEN (Nakarai, Kyoto, Japan) was diluted with 0.9% sodium chloride at a concentration of 200 mg/ml. The CDAA diet and its control, a choline-supplemented, L-amino acid defined (CSAA) diet, with the previously described composition, were obtained from Dyets Inc. (Bethlehem, PA) [28–31]. Oriental MF diet (Oriental Yeast Co. Ltd., Tokyo, Japan) was used as a basal diet. Since 17.8 mg/kg of choline bitarate was contained in 1% (w/w) TJ-9, we added the same amount of choline bitarate to original the CDAA diet and served it for the present studies as previously described [35].

2.3. Animal treatment

The experimental period in all experiments was 16 weeks. In the DEN model, partial hepatectomy (PH) was performed to increase the sensitivity of the bioassay system [38]. The animals in groups 1–3 (G1–G3) and G5 were fed the basal diet throughout the experiment. Groups 1–4 (G1–G4) were administered DEN with a single intraperitoneally injection dose of 200 mg/kg body weight and received PH at week 4. The mice in G1 did not receive any additional treatment as the control group. The mice in G2 and G3 received 20 and 2 mg/kg per day of PE by gavage, respectively. The dose of 2 mg/kg per day has been shown to be a comparable dose to the human clinical dose as described previously [19,32]. In G4, 1% (w/w) of TJ-9 was mixed with the basal diet as described previously [35]. In G5, saline was injected instead of DEN, and subsequent procedure was the same as. It has been shown that PH induces rapid proliferation of hepatocyte and, in turn, enhances the induction of preneoplastic lesion [38]. In this study, we also examined the effect of PH on induction of the preneoplastic lesions (sham-operated group). In the CDAA model, the mice from G6 to G9 received the CDAA diet, and the CSAA diet was given to the mice in G10. In G6, no additional treatment was performed, and served as a control group. Twenty and 2 mg/kg per day PE were administered to G7 and G8, respectively. In G9, the CDAA diet containing 1% (w/w) TJ-9 was given. The samples in the CDAA model were also used for the analysis on liver fibrosis development. All animal procedures were performed according to approved protocols and in accordance with the recommendations for the proper care and use of laboratory animals.

2.4. Histopathological and immunohistochemical examinations

In all experimental groups, 5-μm-thick sections of formalin-fixed and paraffin-embedded livers were processed routinely for hematoxylin and eosin (H&E). In the liver of the CDAA model, Azan–Mallory staining was also employed for determination of the liver fibrosis development. Immunohistochemical staining of two enzyme-altered preneoplastic lesions; namely the placental form of glutathione *S*-transferase (GST-P) and γ-glutamyltransferase (GGT) [39] (Medical and Biological Laboratories Co., Nagoya, Japan) was performed on the liver in both experiments, and α-SMA (DAKO, Kyoto, Japan) staining was also performed on the liver of the CDAA model as described previously [40]. Semi-quantitative analyses of preneoplastic foci, and fibrosis development and immunopositive cell area were carried out with a Fuji-BAS 2000 image analyzing system (Fuji, Tokyo, Japan) as previously described [41]. Regarding the α-SMA-positive cells, we only included in sinusoidal lining for image analysis.

2.5. Hepatic hydroxyproline contents and serum markers

The hepatic hydroxyproline content and the serum marker for fibrosis development, hyaluronic acid were measured as previously described [41]. The alanine aminotransferase aspartate (ALT) and total bilirubin (T. Bil) were assessed using the routine laboratory method.

2.6. The RNA expression of α1-(III) pro-collagen in the liver by real-time PCR

The α1-(III) pro-collagen mRNA expression in the liver of CDAA model was evaluated by real-time polymerase chain reaction (PCR) as described previously [32,42]. The mRNA was extracted from the whole liver of each experimental group from G6 to G10 ($n = 5$). For cDNA synthesis, Taqman reverse transcription reagents were used as described in the manufacturer's manual of the ABI Prism 7700 Sequence Detection System (PE Applied Biosystems, Foster City, CA), which was used for real-time PCR amplification following the Taqman Universal PCR Master Mix Protocol (PE Applied Biosystems). The threshold cycle and the standard curve method were used for calculating the relative amount of the target RNA as

Table 1
Experimental group details given DEN or the CDAA diet with PE or TJ-9[a]

Group	Treatment	Effective no. of rats	Final body weight (g)a	Relative liver weight (g/100 g body wt.)a
1	DEN	10	255 ± 16	2.67 ± 0.21
2	DEN + PE (20 mg/kg)	10	248 ± 18	2.58 ± 0.18
3	DEN + PE (2 mg/kg)	10	251 ± 18	2.51 ± 0.20
4	DEN + TJ-9 (1%)	10	255 ± 20	2.66 ± 0.27
5	PBS	6	261 ± 20	2.77 ± 0.31
6	CDAA	10	265 ± 26	3.12 ± 0.32[b]
7	CDAA + PE (20 mg/kg)	10	264 ± 29	3.14 ± 0.41[b]
8	CDAA + PE (2 mg/kg)	10	265 ± 26	3.12 ± 0.32[b]
9	CDAA + TJ-9 (1%)	10	258 ± 27	3.22 ± 0.33[b]
10	CSAA	6	298 ± 35	2.54 ± 0.14

[a] Data represent mean ± SD.
[b] Statisfically significant different from group 10 ($P < 0.05$).

described for PE. The following temperature was employed: hold 50 °C for 2 min, hold 60 °C for 30 min, hold 94 °C for 5 min, cycle 45 repeats 94 °C for 1 min, 55 °C for 1 min, 72 °C for 1 min. To prevent genomic DNA contamination, all RNA samples were subjected to DNase I digestion and checked by 40 cycles of PCR to confirm the absence of amplified DNA.

2.7. Statistical analysis

To assess the statistical significance of inter-group differences in the quantitative data, Bonferroni's multiple comparison test was performed after one-way analysis of variance followed by Barlett's test to determine the homology of variance.

3. Results

3.1. General findings in the DEN model and CDAA model

Data for the effective numbers of rats, final body weights, relative liver weights in all experimental groups are shown in Table. 1. In the DEN model, there were no significant differences of final body weight and relative liver weight from G1 to G5. On the contrary, in the CDAA models, the final body weight of CDAA-treated rats (G6–G9) was lighter than that of CSAA-treated rats (G10) in accordance with the previous reports [28–31]. The relative liver weights in G6–G9 were greater than in G10. In both models, PE and TJ-9 administration to the PBS- and CSAA-treated rats did not show any change of these markers, respectively. Neither ascites nor other organ abnormalities were observed at the end of the experiment in all groups. PE treatment did not cause any alteration of the serum biochemical markers in both models (data not shown), either.

3.2. Effect of RAS inhibition on the development of preneoplastic lesions in the DEN model and CDAA model

In the DEN model, no histological or biological changes indicating liver injury were observed except the development of preneoplastic foci. The typical microscopic appearance of GST-P-positive foci from G1 is shown in Fig. 1A. As shown in Fig. 2, both of the number and size of preneoplastic foci were significantly suppressed by the treatment of PE and TJ-9 ($P < 0.01$). The clinically comparable low dose (2 mg/kg per day) of PE exerted a similar inhibitory effect on the high dose (20 mg/kg per day) treatment. The

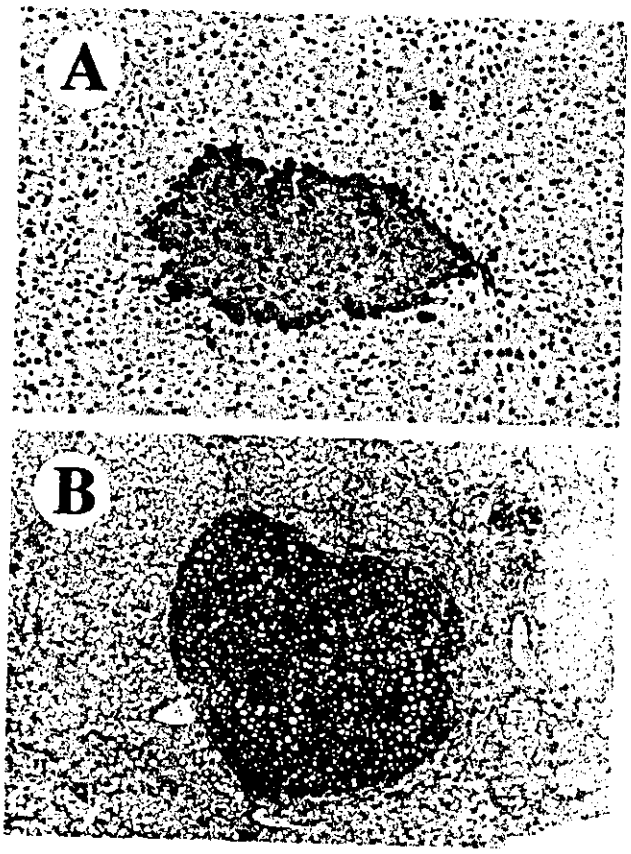

Fig. 1. Representative photomicrographs of GST-P-positive preneoplastic foci in the DEN model (A) and CDAA model (B). In the DEN model, GST-P-positive foci were developed without fibrosis development. On the other hand, GST-P-positive foci induced were surrounded by significant fibrosis septa in the CDAA model. × 100.

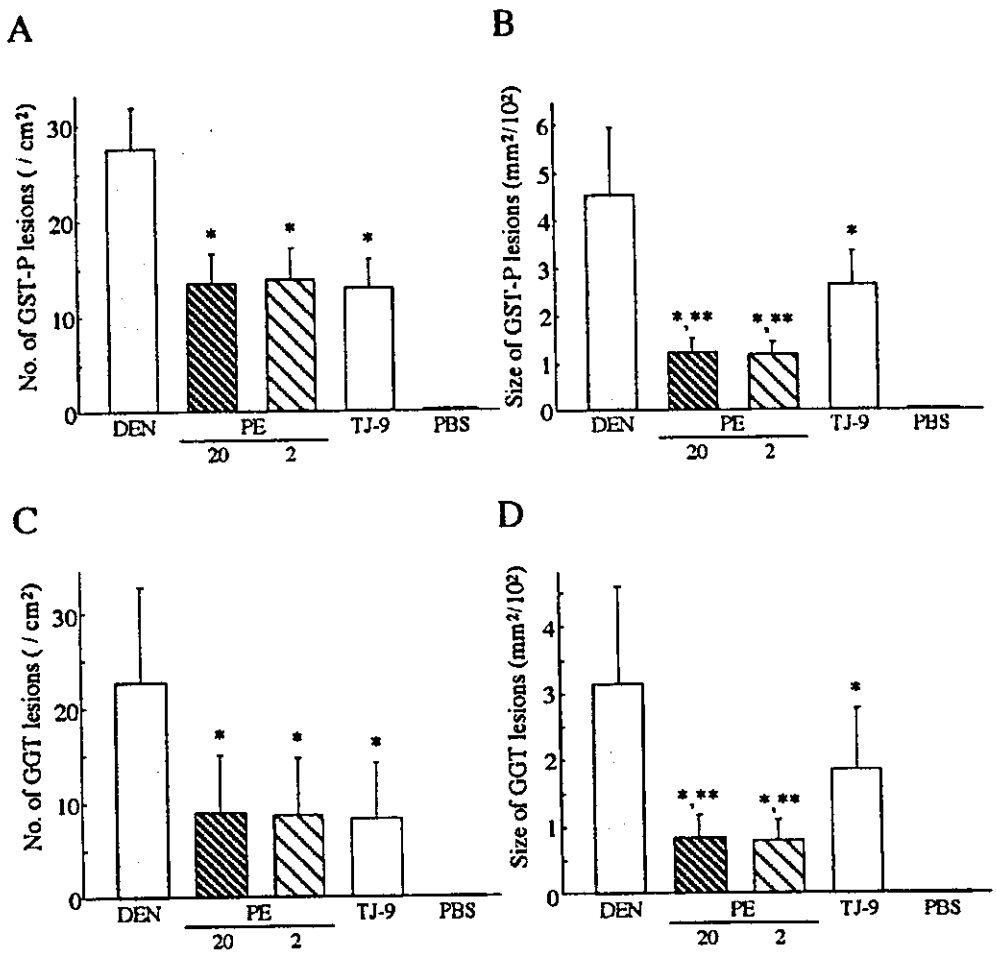

Fig. 2. Effect of PE on the development of DEN-induced GST-P- and GGT-positive preneoplastic foci. Both of number (A) and size (B) of GST-P-positive foci were significantly suppressed by the treatment of PE and TJ-9. The clinically comparable low dose (2 mg/kg per day) of PE exerted a similar inhibitory effect to the high dose (20 mg/kg per day) treatment. The inhibitory effects of the foci development were similar in number in the PE- and TJ-9-treated groups (A), whereas the mean size of GST-P foci in PE-treated groups were significantly smaller than in the TJ-9-treated group (B). No positive foci were found in the PBS-treated group. The results of the GGT-positive lesions were similar to those of the GST-P both in number (C) and size (D). The data represent mean ± SD. Statistically significant difference: *$P < 0.01$ compared with the DEN-treated control group; **$P < 0.05$ compared with the TJ-9-treated group.

inhibitory effects of the foci development in number were of similar magnitude in PE- and TJ-9-treated groups (Fig. 2A). Interestingly, the mean size of GST-P foci in PE-treated groups was significantly smaller than those of the TJ-9-treated group ($P < 0.05$) (Fig. 2B). No positive foci were found in the PBS-treated group. As with GGT-positive preneoplastic foci, similar results were obtained to those of the GST-P (Fig. 2C and D, respectively). As in a previous report [38], the GGT- and GST-P-positive lesions in sham-operated group were markedly lower compared with the PH-performed groups (data not shown).

In the CDAA model, the typical microscopic appearance of GST-P-positive foci induced by the CDAA diet (G6) is shown in Fig. 1B. The PE (20 and 2 mg/kg per day) and TJ-9 treatment significantly attenuated the development of the number of GST-P-positive foci in the livers of CDAA-treated rats (Fig. 3A). These inhibitory effects were also observed in the mean size of GST-P foci (Fig. 3B). As in the DEN model, the size of GST-P foci in the PE-treated group was significantly smaller than that of TJ-9 ($P < 0.05$). In CSAA-treated rats, no GST-P-positive regions were found. As in the DEN model, the results of GGT-positive foci were similar to those of GST-P (Fig. 3C and D, respectively). The immunostaining of the proliferating cell nuclear antigen (PCNA) was not significantly altered in the liver of G1–G4 and groups G6–G9, suggesting that the PE did not affect the hepatocyte proliferation in these models (data not shown).

3.3. Effect of RAS inhibition on CDAA-induced liver fibrosis development

We also examined the effect of PE on CDAA-induced liver fibrosis development. As shown in Fig. 4A, CDAA

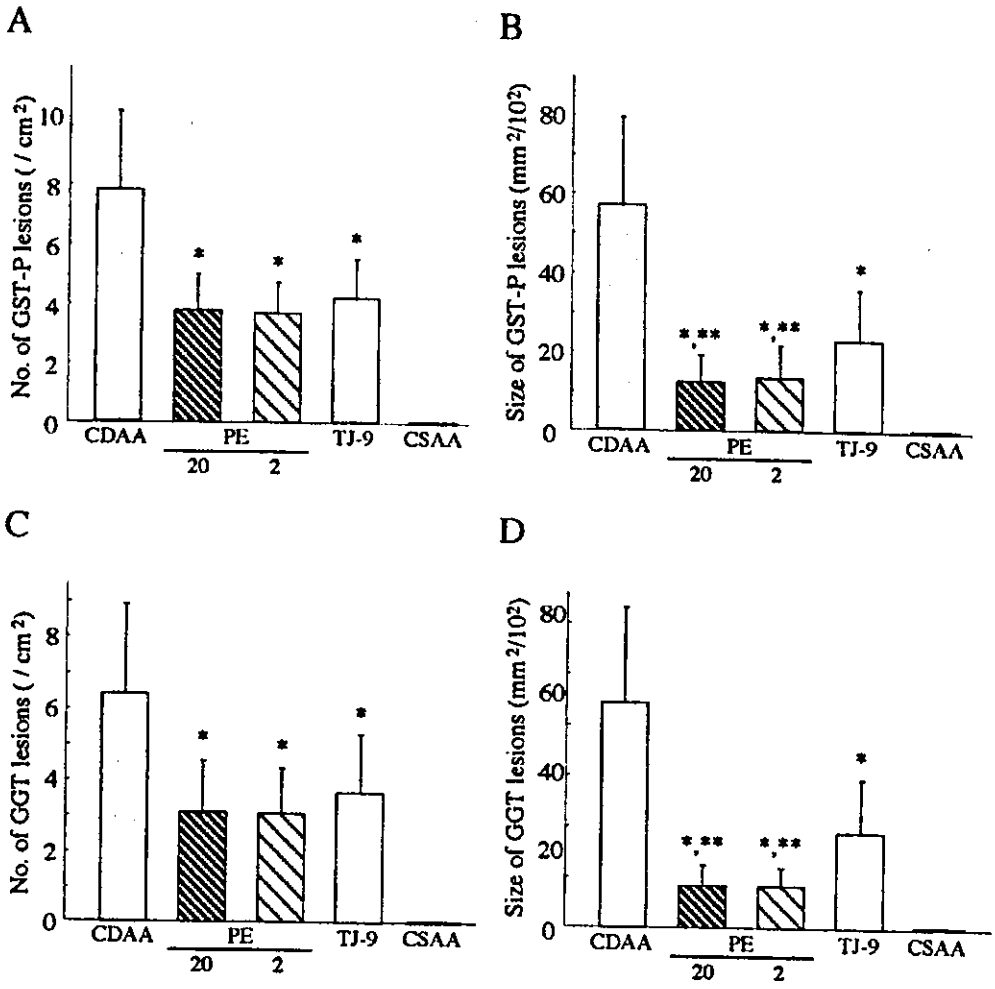

Fig. 3. Effect of PE on the development of GST-P and GGT-positive preneoplastic foci in the CDAA model. The PE and TJ-9 treatment significantly attenuated GST-P-positive foci development both in number (A) and size (B). The low dose (2 mg/kg per day) of PE exerted a similar inhibitory effect on the high dose (20 mg/kg per day) treatment. The numbers of foci development were significantly suppressed by treatment of PE and TJ-9 to a similar extent (A). However, the mean sizes of GST-P foci in PE-treated groups were significantly smaller than those of the TJ-9-treated group (B). In the CSAA diet-treated group, there was no GST-P foci development. The number (C) and size (D) of the GGT-positive lesions were similar to those of the GST-P-positive lesions. The data represent means ± SD. Statistically significant difference: *$P < 0.01$ compared with the CDAA-treated control group; **$P < 0.05$ compared with the TJ-9-treated group.

treatment resulted in a marked liver fibrosis development with fatty accumulation as reported previously [28–31]. The PE (2 mg/kg per day) treatment significantly attenuated liver fibrosis development (Fig. 4B). As shown in Table. 2, a densitometric analysis revealed that the fibrosis areas of PE- (G7 and G8) and TJ-9-treated (G9) groups were less than a half of those of the CDAA-treated control group (G6). The same as with the preneoplastic foci development, 2 mg/kg per day of PE treatment exerted a similar inhibitory effect at the dose of 20 mg/kg per day. The hepatic hydroxyproline content and serum level of hyaluronic acid were also significantly suppressed by treatment with PE and TJ-9 ($P < 0.01$). On the contrary, the serum ALT level did not change by PE and TJ-9 treatment. These results suggested that the inhibitory effect of PE and TJ-9 were not a secondary response to a cytoprotection effect of these agents against CDAA-induced liver injury. We next carried out the immunohistochemical analysis of α-SMA to examine the effect of PE on hepatic stellate cell (HSC) activation during liver fibrosis development. The activated HSC, which express α-SMA and are therefore called myofibroblast-like cells, were drastically reduced in the liver of the PE- and TJ-9-treated groups (Fig. 5A) ($P < 0.01$). We also performed real-time PCR analysis to elucidate the effect of PE on α1-(III) pro-collagen mRNA expression. As shown in Fig. 5B, PE and TJ-9 markedly suppressed mRNA expression of α1-(III) pro-collagen in the liver. The inhibitory effects of PE and TJ-9 on α-SMA, and α1-(III) pro-collagen mRNA expressions exerted mostly parallel reductions. These results suggested that the anti-fibrotic effect of these agents were achieved by the suppression of HSC activation.

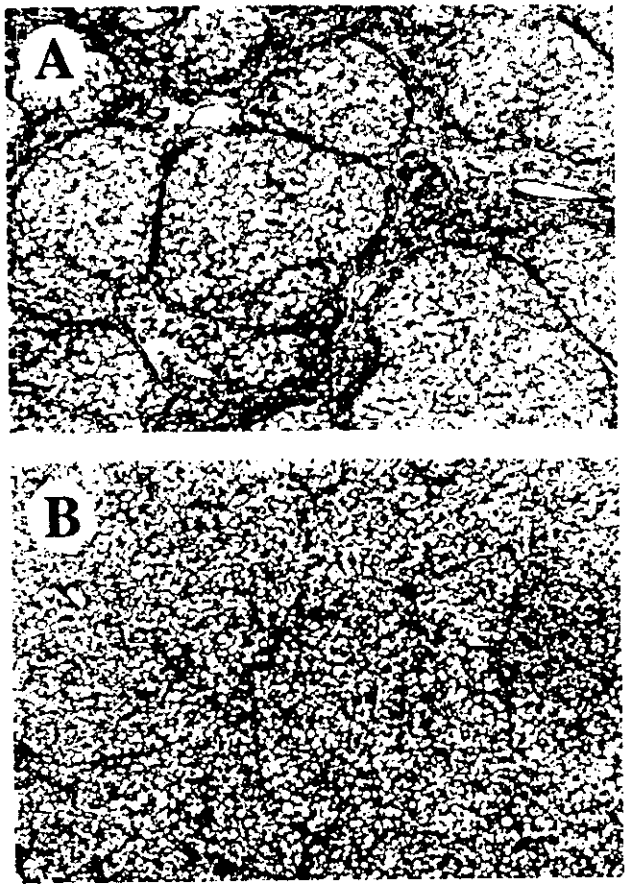

Fig. 4. Microphotographs of liver sections from the CDAA diet-treated rats (A) and CDAA plus PE (2 mg/kg per day)-treated rats (B). The CDAA treatment showed an extensive fibrosis development with fatty accumulations, and the low dose of PE treatment significantly attenuated the fibrogenesis. (Azan–Mallory staining, original magnification ×40).

4. Discussion

The present study revealed that the inhibition of renin angiotensin system (RAS) by clinically used ACE inhibitor (ACE-I), perindopril (PE), significantly attenuated the hepatic preneoplastic foci in two different liver carcinogenesis models. PE also markedly inhibited the liver fibrogenesis associated with the suppression of HSC.

HCC is one of the most common malignancies in the world with an estimated annual incidence of greater than 1 million new cases per year [43]. Although several alternative therapies other than radical operation have been employed such as a transarterial embolization, there is still no satisfactory improvement in the prognosis of HCC to date [43–46]. One of the reasons for the poor prognosis of HCC is the high rate of recurrence. This high recurrence rate, even after curative therapy, has been shown to be due to intrahepatic metastasis or multicentric development of each respective neoplasm clone [44–46]. It has been shown that the existence of liver fibrotic changes promotes hepatocarcinogenesis [47]. Since the high-risk group of HCC development seems to be clearer than other types of tumor, it is likely that a primary or secondary chemopreventive agent would be beneficial in improving the prognosis of HCC. Several agents, such as interferon and acyclic retinoid, have been shown to prevent secondary HCC recurrence; however, there are still problems for common clinical application with its expense and long term toxicity [48,49]. We found that PE significantly inhibited the hepatic preneoplastic foci at a clinically comparable low dose. A retrospective cohort study of 5207 patients receiving ACE-I or other hypertensive drugs with a 10-year follow-up has shown that ACE-I treatment may decrease the incidence of adult cancer and fetal cancer [50]. ACE-I is already widely used as an anti-hypertensive agent without serious side effects. Taken together, it may thus be possible that PE can be utilized as a chemopreventive agent against HCC. In this study, we used two different rat hepatocarcinogenesis models, namely, the DEN model and CDAA model. In the DEN and CDAA models, HCC is induced through the development of preneoplastic foci without and with cirrhosis, respectively [25–31]. To evaluate the effect of PE, we used the GST-P- and GGT-positive preneoplastic foci as end points in the current study. However, it has been shown that TJ-9 did not prevent the HCC development in the LEC rat model although it suppressed the preneoplastic foci in the DEN and CDAA models [35,37,51]. Further long-term studies are required to elucidate whether PE can really prevent HCC development. Also, it is important to elucidate whether PE attenuated the cell transformation, or influenced the preneoplastic foci growth in the future.

Interestingly, we found that the inhibitory effect of PE on the size of preneoplastic foci was significantly smaller than

Table 2
Effect of PE and TJ-9 on various markers in the CDAA diet-treated rats[a]

Group	Treatment	Fibrosis area (mm^2 liver)	Hydroxyproline (μg/g wet liver)	Hyaluronic acid (ng/ml)	ALT (U/l)
6	CDAA	1.38 ± 0.31	621 ± 154	82 ± 32	128 ± 62
7	CDAA + PE (20 mg/kg)	0.54 ± 0.22[b]	243 ± 121[b]	34 ± 16[b]	120 ± 56
8	CDAA + PE (2 mg/kg)	0.47 ± 0.21[b]	228 ± 132[b]	33 ± 17[b]	131 ± 72
9	CDAA + TJ-9 (1%)	0.61 ± 0.30[b]	301 ± 142[b]	40 ± 21[b]	117 ± 64
10	CSAA	0.05 ± 0.01	57 ± 22	17 ± 8	22 ± 6

[a] Data represent mean ± SD ($n = 10$).
[b] Statistically different from group 6 ($P < 0.01$).

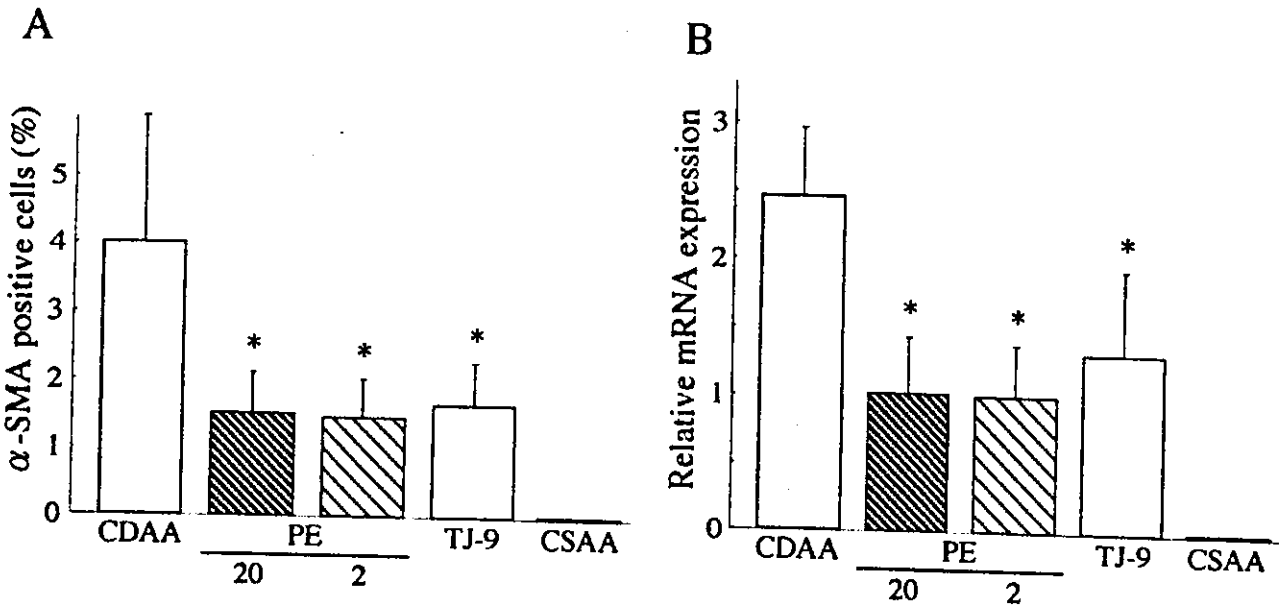

Fig. 5. Densitometric analysis of α-SMA-positive cells (A) and α-(III) pro-collagen mRNA expression (B) in the CDAA diet-treated liver. The α-SMA-positive activated HSC and α-(III) pro-collagen mRNA were significantly suppressed by PE and TJ-9 treatment. The inhibitory effects of PE and TJ-9 on α-SMA and α1-(III) pro-collagen expressions exerted mostly parallel reductions. In the PE-treated groups, 20 and 2 represent 20 mg/kg and 2 mg/kg per day treatment of PE, respectively. The data represent means ± SD. Statistically significant difference: *$P < 0.01$ compared with the CDAA-treated control group.

that of TJ-9, although very similar in number. Until recently, it had been believed that angiogenesis starts at a size of several hundred microns to 1 mm in diameter or when the tumor contains roughly 10^5–10^6 cells [52]. It has been recently proven that angiogenesis has already begun at a very early stage when the tumor contained just 100–300 cells [53]. As described, it is suggested that angiogenesis is now involved in the early carcinogenesis step [24–26]. A recent study of the endothelial cell marker in dysplastic lesions of the liver suggested that alterations in the hepatic microcirculation already occur at very early stages of liver carcinogenesis [54]. Since PE has been shown to possess anti-angiogenic activity [19], the smaller size of preneoplastic foci in the PE-treated group may be attributed to the anti-angiogenic activity. The direct interaction of PE treatment and the angiogenesis development during hepatocarcinogenesis is currently being evaluated at our laboratory.

AT-II has also been considered a potential mediator of liver fibrosis development [3–7,9]. It has been shown that AT-II induced contraction of proliferation of activated human HSC [9]. In this study, we found that RAS inhibition by PE significantly attenuated CDAA-induced liver fibrogenesis. The PE treatment markedly suppressed the number of α-SMA-positive cells and α1-(III) pro-collagen mRNA expression, suggesting that this anti-fibrotic effect by RAS inhibition using PE was result of the suppression of HSC activation. As with the development of preneoplastic foci, this anti-fibrotic effect was achieved at the clinically comparable low dose (2 mg/kg per day). We previously found that PE treatment attenuated pig serum-induced liver fibrosis development [32], suggesting that the anti-fibrotic effect of PE was not experimental model-specific but a general phenomenon.

In summary, we found that the RAS played a pivotal role in liver carcinogenesis and fibrogenesis. The clinically comparable dose of ACE-I, PE, significantly attenuated the liver preneoplastic foci and liver fibrosis development. Since PE is widely used in clinical practice without serious side effects, it may provide an effective new strategy for anti-hepatocarcinogenesis chemoprevention and fibrosis therapies.

References

[1] Dzau VJ, Gibbons GH, Pratt RE. Molecular mechanisms of vascular renin–angiotensin system in myointimal hyperplasia. Hypertension 1991;18:II100–II105.
[2] Matsusaka T, Ichikawa I. Biological functions of angiotensin and its receptors. Annu Rev Physiol 1997;59:395–412.
[3] Schneider AW, Kalk JF, Klein CP. Effect of losartan, an angiotensin II receptor antagonist, on portal pressure in cirrhosis. Hepatology 1999;29:334–339.
[4] Arroyo V, Bosch J, Mauri M, Ribera F, Navarro-Lopez F, Rodes J. Effect of angiotensin-II blockade on systemic and hepatic haemodynamics and on the renin–angiotensin-aldosterone system in cirrhosis with ascites. Eur J Clin Invest 1981;11:221–229.
[5] Helmy A, Jalan R, Newby DE, Hayes PC, Webb DJ. Role of angiotensin II in regulation of basal and sympathetically stimulated vascular tone in early and advanced cirrhosis. Gastroenterology 2000;118:565–572.
[6] Garcia-Pagan JC, Bosch J, Rodés J. The role of vasoactive mediators in portal hypertension. Semin Gastrointest Dis 1995;6:140–147.
[7] Ballet F, Chretien Y, Rey C, Poupon R. Differential response of normal and cirrhotic liver to vasoactive agents. A study in the isolated perfused rat liver. J Pharmacol Exp Ther 1988;244:283–289.

[8] Friedman SL. Cytokines and fibrogenesis. Semin Liver Dis 1999;19:129–140.
[9] Bataller R, Ginès P, Nicolas JM, Gorbig MN, Garcia-Ramallo E, Gasull X, et al. Angiotensin II induces contraction and proliferation of human hepatic stellate cells. Gastroenterology 2000;118:1149–1156.
[10] Le Noble FA, Hekking JW, Van Straaten HW, Slaaf DW, Struyker Boudier HA. Angiotensin II stimulates angiogenesis in the chorio-allantoic membrane of the chick embryo. Eur J Pharmacol 1991;195:305–306.
[11] Fernandez LA, Twickler J, Mead A. Neovascularization produced by angiotensin II. J Lab Clin Med 1985;105:141–145.
[12] Pupilli C, Lasagni L, Romagnani P, Bellini F, Mannelli M, Misciglia N, et al. Angiotensin II stimulates the synthesis and secretion of vascular permeability factor/vascular endothelial growth factor in human mesangial cells. J Am Soc Nephrol 1999;10:245–255.
[13] Hori K, Saito S, Takahashi H, Sato H, Maeda H, Sato Y. Tumor-selective blood flow decrease induced by an angiotensin converting enzyme inhibitor, temocapril hydrochloride. Jpn J Cancer Res 2000;91:261–269.
[14] Folkman J. Angiogenesis in cancer, vascular, rheumatoid and other disease. Nat Med 1995;1:27–31.
[15] Fidler IJ, Ellis LM. The implications of angiogenesis for the biology and therapy of cancer metastasis. Cell 1994;79:185–188.
[16] Ferrara N, Alitalo K. Clinical applications of angiogenic growth factors and their inhibitors. Nat Med 1999;5:1359–1364.
[17] Suzuki K, Hayashi N, Miyamoto Y, Yamamoto M, Ohkawa K, Ito Y, et al. Expression of vascular permeability factor/vascular endothelial growth factor in human hepatocellular carcinoma. Cancer Res 1996;56:3004–3009.
[18] Mise M, Arii S, Higashituji H, Furutani M, Niwano M, Harada T, et al. Clinical significance of vascular endothelial growth factor and basic fibroblast growth factor gene expression in liver tumor. Hepatology 1996;23:455–464.
[19] Yoshiji H, Kuriyama S, Kawata M, Yoshii J, Ikenaka Y, Noguchi R, et al. The angiotensin-I-converting enzyme inhibitor perindopril suppresses tumor growth and angiogenesis: possible role of the vascular endothelial growth factor. Clin Cancer Res 2001;7:1073–1078.
[20] Kardum D, Huskic J, Fabijanic D, Banic M, Buljevac M, Kujundzic M, et al. Activity of serum angiotensin-converting enzyme as a tumour marker of hepatocellular carcinoma. Eur J Gastroenterol Hepatol 1999;11:1209–1213.
[21] Bolontrade MF, Stern MC, Binder RL, Zenklusen JC, Gimenez-Conti IB, Conti CJ. Angiogenesis is an early event in the development of chemically induced skin tumors. Carcinogenesis 1998;19:2107–2113.
[22] Bergers G, Javaherian K, Lo KM, Folkman J, Hanahan D. Effects of angiogenesis inhibitors on multistage carcinogenesis in mice. Science 1999;284:808–812.
[23] Brandvold KA, Neiman P, Ruddell A. Angiogenesis is an early event in the generation of myc-induced lymphomas. Oncogene 2000;19:2780–2785.
[24] Mazzanti R, Messerini L, Monsacchi L, Buzzelli G, Zignego AL, Foschi M, et al. Chronic viral hepatitis induced by hepatitis C but not hepatitis B virus infection correlates with increased liver angiogenesis. Hepatology 1997;25:229–234.
[25] Tamura K, Nakae D, Horiguchi K, Akai H, Kobayashi Y, Andoh N, et al. Inhibition by *N*-(4-hydroxyphenyl)retinamide and all-*trans*-retinoic acid of exogenous and endogenous development of putative preneoplastic, glutathione *S*-transferase placental form-positive lesions in the livers of rats. Carcinogenesis 1997;18:2133–2141.
[26] Pegg AE. Formation and metabolism of alkylated nucleosides: possible role in carcinogenesis by nitroso compounds and alkylating agents. Adv Cancer Res 1977;25:195–269.
[27] Saffhill R, Margison GP, O'Connor PJ. Mechanisms of carcinogenesis induced by alkylating agents. Biochim Biophys Acta 1985;823:111–145.
[28] Nakae D, Yoshiji H, Mizumoto Y, Horiguchi K, Shiraiwa K, Tamura K, et al. High incidence of hepatocellular carcinomas induced by a choline deficient L-amino acid defined diet in rats. Cancer Res 1992;52:5042–5045.
[29] Endoh T, Tang Q, Denda A, Noguchi O, Kobayashi E, Tamura K, et al. Inhibition by acetylsalicylic acid, a cyclo-oxygenase inhibitor, and p-bromophenacylbromide, a phospholipase A2 inhibitor, of both cirrhosis and enzyme-altered nodules caused by a choline-deficient, L-amino acid-defined diet in rats. Carcinogenesis 1996;17:467–475.
[30] Denda A, Tang Q, Endoh T, Tsujiuchi T, Horiguchi K, Noguchi O, et al. Prevention by acetylsalicylic acid of liver cirrhosis and carcinogenesis as well as generations of 8-hydroxydeoxyguanosine and thiobarbituric acid-reactive substances caused by a choline-deficient, -amino acid-defined diet in rats. Carcinogenesis 1994;15:1279–1283.
[31] Yoshiji H, Nakae D, Mizumoto Y, Horiguchi K, Tamura K, Denda A, et al. Inhibitory effect of dietary iron deficiency on inductions of putative preneoplastic lesions as well as 8-hydroxydeoxyguanosine in DNA and lipid peroxidation in the livers of rats caused by exposure to a choline-deficient L-amino acid defined diet. Carcinogenesis 1992;13:1227–1233.
[32] Yoshiji H, Kuriyama S, Yoshii J, Ikenaka Y, Noguchi R, Nakatani T, et al. Angiotensin-II type 1 receptor interaction is a major regulator for liver fibrosis in rats. Hepatology 2001;34:745–750.
[33] Jonsson JR, Clouston AD, Ando Y, Kelemen LI, Horn MJ, Adamson MD, et al. Angiotensin-converting enzyme inhibition attenuates the progression of rat hepatic fibrosis. Gastroenterology 2001;121:148–155.
[34] Ohishi T, Saito H, Tsusaka K, Toda K, Inagaki H, Hamada Y, et al. Anti-fibrogenic effect of an angiotensin converting enzyme inhibitor on chronic carbon tetrachloride-induced hepatic fibrosis in rats. Hepatol Res 2001;21:147–158.
[35] Sakaida I, Matsumura Y, Akiyama S, Hayashi K, Ishige A, Okita K. Herbal medicine Sho-saiko-to (TJ-9) prevents liver fibrosis and enzyme-altered lesions in rat liver cirrhosis induced by a choline-deficient L-amino acid-defined diet. J Hepatol 1998;28:298–306.
[36] Oka H, Yamamoto S, Kuroki T, Harihara S, Marumo T, Kim SR, et al. Prospective study of chemoprevention of hepatocellular carcinoma with Sho-saiko-to (TJ-9). Cancer 1995;76:743–749.
[37] Okita K, Kurokawa F, Yamasaki T. Possible prevention of hepatocarcinogenesis with Sho-saiko-to. Gastroenterology (Tokyo) 1990;12:152–156.
[38] Ito N, Tatematsu M, Hasegawa R, Tsuda H. Medium-term bioassay system for detection of carcinogens and modifiers of hepatocarcinogenesis utilizing the GST-P positive liver cell focus as an endpoint marker. Toxicol Pathol 1989;17:630–641.
[39] Obara T, Makino T, Ura H, Yokose Y, Kinugasa T, Moore MA, et al. Comparative histochemical investigation of the glutathione *S*-transferase placental form and gamma-glutamyltranspeptidase during *N*-nitrosobis(2-hydroxypropyl)amine-induced pancreatic carcinogenesis in hamsters. Carcinogenesis 1986;7:801–805.
[40] Yoshiji H, Harris SR, Raso E, Gomez DE, Lindsay CK, Shibuya M, et al. Mammary carcinoma cells over-expressing tissue inhibitor of metalloproteinases-1 show enhanced vascular endothelial growth factor expression. Int J Cancer 1998;75:81–87.
[41] Yoshiji H, Kuriyama S, Miyamoto Y, Thorgeirsson UP, Gomez DE, Kawata M, et al. Tissue inhibitor of metalloproteinases-1 promotes liver fibrosis development in a transgenic mouse model. Hepatology 2000;32:1248–1254.
[42] Nagao M, Nakajima Y, Kanehiro H, Hisanaga M, Aomatsu Y, Ko S, et al. The impact of interferon gamma receptor expression on the mechanism of escape from host immune surveillance in hepatocellular carcinoma. Hepatology 2000;32:491–500.
[43] Schafer DF, Sorrell MF. Hepatocellular carcinoma. Lancet 1999;353:1253–1257.
[44] Yamanaka N, Okamoto E, Toyosaka A, Mitunobu M, Fujihara S, Kato T, et al. Prognostic factors after hepatectomy for hepatocellular carcinomas. A univariate and multivariate analysis. Cancer 1990;65:1104–1110.

[45] Arii S, Tanaka J, Yamazoe Y, Minematsu S, Morino T, Fujita K, et al. Predictive factors for intrahepatic recurrence of hepatocellular carcinoma after partial hepatectomy. Cancer 1992;69:913–919.
[46] Ikeda K, Saitoh S, Tsubota A, Arase Y, Chayama K, Kumada H, et al. Risk factors for tumor recurrence and prognosis after curative resection of hepatocellular carcinoma. Cancer 1993;71:19–25.
[47] Sakaida I, Hironaka K, Uchida K, Suzuki C, Kayano K, Okita K. Fibrosis accelerates the development of enzyme-altered lesions in the rat liver. Hepatology 1998;28:1247–1252.
[48] Ikeda K, Arase Y, Saitoh S, Kobayashi M, Suzuki Y, Suzuki F, et al. Interferon beta prevents recurrence of hepatocellular carcinoma after complete resection or ablation of the primary tumor – a prospective randomized study of hepatitis C virus-related liver cancer. Hepatology 2000;32:228–232.
[49] Muto Y, Moriwaki H, Ninomiya M, Adachi S, Saito A, Takasaki KT, et al. Prevention of second primary tumors by an acyclic retinoid, polyprenoic acid, in patients with hepatocellular carcinoma. Hepatoma Prevention Study Group. N Engl J Med 1996;334:1561–1567.
[50] Lever AF, Hole DJ, Gillis CR, McCallum IR, McInnes GT, MacKinnon PL, et al. Do inhibitors of angiotensin-I-converting enzyme protect against risk of cancer? Lancet 1998;352:179–184.
[51] Watanabe S, Kitade Y, Masaki T, Nishioka M, Satoh K, Nishino H. Effects of lycopene and Sho-saiko-to on hepatocarcinogenesis in a rat model of spontaneous liver cancer. Nutr Cancer 2001;39:96–101.
[52] Folkman J. Tumor angiogenesis: therapeutic implications. N Engl J Med 1971;285:1182–1186.
[53] Li CY, Shan S, Huang Q, Braun RD, Lanzen J, Hu K, et al. Initial stages of tumor cell-induced angiogenesis: evaluation via skin window chambers in rodent models. J Natl Cancer Inst 2000;92:143–147.
[54] Frachon S, Gouysse G, Dumorti J, Couvelard A, Nejjari M, Mion F, et al. Endothelial cell marker expression in dysplastic lesions of the liver: an immunohistochemical study. J Hepatol 2001;34:850–857.

ORIGINAL ARTICLE

Taylor & Francis
healthsciences

Expression of $p33^{ING1}$ in Hepatocellular Carcinoma: Relationships to Tumour Differentiation and Cyclin E Kinase Activity

T. Ohgi, T. Masaki, S. Nakai, A. Morishita, S. Yukimasa, M. Nagai, Y. Miyauchi, T. Funaki, K. Kurokohchi, S. Watanabe & S. Kuriyama
Third and First Depts. of Internal Medicine, Kagawa Medical University, Miki-cho, Kita-gun, Kagawa, Japan

Ohgi T, Masaki T, Nakai S, Morishita A, Yukimasa S, Nagai M, Miyauchi Y, Funaki T, Kurokohchi K, Watanabe S, Kuriyama S. Expression of $p33^{ING1}$ in hepatocellular carcinoma: relationships to tumour differentiation and cyclin E kinase activity. Scand J Gastroenterol 2002;37:1440–1448.

Background: Inhibitor of growth-1 (ING1) is a new candidate for the tumour suppressor gene that encodes a 33k Da protein ($p33^{ING1}$). While reduction of $p33^{ING1}$ is an important event in some human cancers, the expression of $p33^{ING1}$ in human hepatocellular carcinoma (HCC) remains to be examined. We evaluated $p33^{ING1}$ expression in various liver diseases including HCC. **Methods:** Expression of $p33^{ING1}$ was evaluated immunohistochemically not only in the normal liver ($n = 5$), but also in specimens of chronic hepatitis ($n = 39$) and HCC ($n = 86$). We also analysed the relationship between $p33^{ING1}$ expression and cyclin E kinase activity detected by autoradiography in 29 HCCs. **Results:** Expression of $p33^{ING1}$ was reduced in HCC, especially in moderately and poorly differentiated HCCs, and those at advanced stages. Furthermore, expression of $p33^{ING1}$ correlated inversely with cyclin E kinase activity. **Conclusions:** These data suggest that reduction of $p33^{ING1}$ may contribute to the process of malignant transformation, progression and dedifferentiation of HCC via an increase of cyclin E kinase activity.

Key words: Cyclin E; differentiation; hepatocellular carcinoma; $p33^{ING1}$

Shigeki Kuriyama, M.D., Ph.D., Third Dept. of Internal Medicine, Kagawa Medical University, 1750-1, Ikenobe, Miki-cho, Kita-gun, Kagawa, 761-0793, Japan (fax. +81 878 891 2158, e-mail. skuriyam@kms.ac.jp)

Among a number of tumour suppressor genes, p53 and Rb tumour suppressors are of key importance in the genetic aetiology of hepatocellular carcinoma (HCC) (1). Loss of p53 function results in inappropriate cell cycle progression, uncontrolled growth and tumourigenesis (2). However, the role of other tumour suppressor genes in hepatocarcinogenesis remains unknown.

The $p33^{ING1}$ protein has recently been isolated using a method of combined subtractive hybridization of cDNAs from normal and neoplastic cells with an in vivo selection assay (3). The corresponding gene, termed inhibitor of growth 1 (ING1), encodes $p33^{ING1}$, as a 33 kDa nuclear protein that contains a zinc-finger motif (4). It has been shown that expression of $p33^{ING1}$ is up-regulated in senescent fibroblasts, and that its overexpression inhibits cell growth by arresting cells in the G1 phase of the cell cycle as well as promoting apoptosis (5–7). Interestingly, $p33^{ING1}$ induces the gene encoding $p21^{WAF1}$, which mediates p53-dependent growth arrest. A recent study indicated that $p33^{ING1}$ directly cooperated with p53 in growth regulation by modulating the ability of p53 to act as a transcriptional activator (5). The $p33^{ING1}$ gene has been mapped to chromosome 13q in region 33 to 34 (8), where translocation or deletion has been found in various cancers, including HCC (9–11). In addition, reduced $p33^{ING1}$ expression has been reported in breast cancer, gastric cancer, neck cancer and malignant lymphoma in various studies, including our own (12–16). These observations also indicate that inactivation of $p33^{ING1}$ might be related to the development or progression of HCC.

Since the role of $p33^{ING1}$ in human hepatocarcinogenesis has not been elucidated, we analysed $p33^{ING1}$ expression immunohistochemically in HCC, and examined the relationship between $p33^{ING1}$ expression and the activity of cyclin E kinase, a well-established marker of cell proliferation that accelerates the G1 phase of the cell cycle (17). This study is the first report to assess the involvement of $p33^{ING}$ in hepatocarcinogenesis.

Patients and Methods

Patients

Tissue samples were obtained by surgical resection or liver biopsy from 86 patients with HCC (61 m, 25 f; mean age 63.0 ± 8.6 years, range, 34–80). Of the 86 patients, 77 were positive for hepatitis C virus (HCV)-RNA and 9 were positive for hepatitis B surface antigen (HBs Ag). According to the pathologic tumour-nodes-metastasis (pTNM) classification proposed by the International Union Against Cancer and the

Table I. Characteristics of patients with HCC

Gender	
Male	61
Female	25
Age (years)	
Mean ± s	63.0 ± 8.6
Range	34–80
Viral infection	
HCV-positive	77
HBsAg-positive	9
Histological background	
Normal liver	0
F1	0
F2	3
F3	11
F4	72
Histological grade[a]	
WD	17
MD	59
PD	10
TNM stage[b]	
I	16
II	17
III	15
IVA and IVB	38
AFP concentration in serum	
Normal	19
Elevated	67
Mean s (ng/mL)	22426 ± 92604
Range (ng/mL)	2.0–787000

[a] Histological grading of HCC was determined using the criteria of the Internal Working Party.

[b] TNM stage was determined using the classification proposed by the Internal Union Against Cancer and American Joint Committee on cancer.

Abbreviations: HCC = hepatocellular carcinoma; HCV = hepatitis C virus; HBs Ag = hepatitis B surface antigen; WD = well differentiated; MD = moderately differentiated; PD = poorly differentiated; AFP = α-fetoprotein; s = standard deviation.

American Joint Committee on Cancer (UICC, 1997), 16 patients were in stage I, 17 in stage II, 15 in stage III, 29 in stage IVA and 9 in stage IVB. HCCs were classified as well differentiated, moderately differentiated or poorly differentiated according to the criteria proposed by the International Working Party (18); this grading was based on the predominant findings in the sections of the worst-appearing area. Clinical and biochemical data about the patients with HCC are presented in Table I. All cases were studied immunohistochemically and 29 were also assayed for cyclin E kinase activity. Tissues were obtained by liver biopsy from 44 patients with chronic hepatitis, including 31 HCV-RNA-positive cases, 8 HBs Ag-positive cases and 5 cases negative for both. According to Desmet's classification (19) of fibrosis, the chronic hepatitis cases included 7 in fibrosis stage F1, 14 in F2, 11 in F3 and 12 in F4. Clinical and biochemical data concerning the patients with chronic hepatitis are presented in Table II. Five normal liver samples were obtained during surgery for colon cancer with liver metastasis. These patients were negative for both HCV-RNA and HBs Ag. The normal samples were subjected to both immunohistochemical analysis and the cyclin E kinase assay.

Table II. Characteristics of patients with chronic hepatitis

Gender	
Male	27
Female	12
Age (years)	
Mean ± s	50.9 ± 13.4
Range	21–80
Viral infection	
HCV-positive	31
HBs Ag-positive	8
ALT concentration in serum	
Normal	4
Elevated	35
Mean ± s (IU/L)	74.3 ± 35.5
Range	14–187
Fibrosis stage[a]	
F1	7
F2	9
F3	11
F4	12

[a] The fibrosis stage was assessed using Desmet's classification.

Abbreviations: ALT = alanine-transferase; HBs Ag = hepatitis B surface antigen; HCV = hepatitis C virus; s = standard deviation.

Reagents and antibodies

Reagents were obtained from Sigma Chemical (Tokyo, Japan) or Wako Pure Chemical (Tokyo, Japan). Anti-$p33^{ING1}$ monoclonal antibody was raised against a glutathione S-transferase (GST) fusion protein, partly encoded by an isolated cDNA for $p33^{ING1}$ (7). Cyclin E polyclonal antibody (clone M-20; Santa Cruz Biotechnology, Tokyo, Japan) was raised against the epitope consisting of amino acids 378 to 396 at the carboxy terminus of rat cyclin E; this antibody reacts with mouse, rat and human cyclin E. The optimal dilution of $p33^{ING1}$ antibody for the immunohistochemical in this study was determined to be 1:100.

Immunohistochemical examination

We prepared 2-μm-thick sections from formalin-fixed, paraffin-embedded tissue blocks. Sections were stained by an avidin-biotin-peroxidase complex (ABC) method (Funakoshi Chemical, Tokyo, Japan) (20). For detection of $p33^{ING1}$, sections were placed in 10 nmol/L citrate buffer (pH 6.0) and processed at 500 W at 95 °C for 10 min in a microwave oven (RE-M20 Microwave Processor; Sharp, Osaka, Japan). Sections were deparaffinized in xylene, rehydrated in a graded series of alcohol solutions, and then mixed with a solution containing 0.5% hydrogen peroxidase to block endogenous peroxidase activity. After washing with phosphate-buffered saline (PBS), sections were processed for immunostaining by the ABC method. Primary incubation was performed overnight at 24 °C with monoclonal antibody against $p33^{ING1}$. As a negative control, non-immune mouse IgG was substituted for the primary antibody. For signal amplification, the Renaissance TSA amplification kit (NEN Life Science Products, Boston, USA) was used (21). Diaminobenzidine was used as the chromogen.

All sections were examined independently by two pathol-

Table III. Patient characteristics and histological features of HCC analysed for cyclin E kinase

Patient no.	Age	Gender	Viral infection	Histological background[a]	TNM stage[b]	Histological grade[c]	AFP (ng/ml)	$p33^{ING1}$ staining pattern
1	67	F	C	F4	I	WD	14	N
2	65	M	C	F4	I	WD	20	N
3	54	F	C	F4	I	WD	575	C
4	64	M	C	F4	II	WD	26	N
5	68	F	C	F4	II	MD	1080	N
6	65	F	C	F4	I	MD	59	N
7	70	M	C	F4	I	MD	38	N
8	61	M	C	F4	II	MD	23	—
9	71	M	C	F3	II	MD	4	N
10	58	M	C	F4	II	MD	10	—
11	67	F	C	F4	II	MD	2350	C
12	60	M	C	F4	II	MD	100	-
13	68	M	C	F4	III	MD	233000	C
14	80	F	C	F4	III	MD	270	—
15	66	M	B	F4	III	MD	7	—
16	75	M	C	F4	IVA	MD	43700	N
17	58	M	C	F4	IVA	MD	86	—
18	61	F	B	F4	IVA	MD	10300	C
19	54	M	C	F3	IVA	MD	41990	—
20	58	M	C	F4	IVA	MD	5	—
21	34	M	B	F4	IVA	MD	1620	C
22	58	M	B	F3	IVA	MD	14	N
23	59	F	B	F3	IVA	MD	2160	N
24	66	F	C	F4	IVB	MD	19600	—
25	55	M	C	F4	II	PD	6100	—
26	77	M	C	F4	IVA	PD	5400	—
27	53	F	C	F4	IVA	PD	66	—
28	56	M	C	F4	IVA	PD	170000	—
29	67	M	C	F4	IVB	PD	7510	—

[a] The fibrosis stage of tissue surrounding HCC was assessed using Desmet's classification.
[b] TNM classification was determined by the criteria proposed by the International Union Against Cancer and American Joint Committe on Cancer.
[c] Histological grading of HCC followed the criteria of the Liver Cancer Study Group of Japan.
Abbreviations: M = male; F = female; B = hepatitis B virus; C = hepatitis C virus; WD = well differentiated; MD = moderately differentiated; PD = poorly differentiated; AFP = α-fetoprotein; N = nuclear staining; C = cytoplasmic staining; — = no staining.

ogists (T.M., S.W.) who were unaware of the clinical information about the case. In each case, the predominant staining pattern for $p33^{ING1}$ was classified as negative, cytoplasmic or nuclear. Nuclear and cytoplasmic staining of $p33^{ING1}$ protein was graded as no detectable expression (a), faint expression (b; present in fewer than 10% of hepatocytes or cancer cells), moderate expression (c; present in 10% to 50% of hepatocytes or cancer cells), or strong expression (d; present in over 50% of hepatocytes or cancer cells). For analysis, the (a) and (b) subgroups were combined as 'negative', while subgroups (c) and (d) were combined as 'positive'.

Tissue lysates

Among the HCC samples obtained at surgery, 29 were frozen in dry ice within 20 min of collection, and subsequently homogenized in a lysis buffer (50 mM N-2-hydroxyethylpiperazine-N'-2-ethanesulfonic acid (HEPES; pH 7.0), 250 mM NaCl, 0.1% Nonidet P-40, 100 mM NaF, 200 mM sodium orthovanadate, 0.5 mM phenylmethylsulfonyl fluoride (PMSF) and 10 μg/ml aprotinin). Lysates were centrifuged at 29,000 g for 20 min at 4 °C. Protein concentration was measured using a dye-binding assay. Protein concentration was measured by the dye-binding protein assay according to the method of Bradford. The lysates were used for the kinase assay and Western blot of cyclin E. Clinical and biochemical data of the patients studied are presented in Table III.

Measurement of cyclin E kinase activity

In *Escherichia coli*, pRb was expressed as a 46 kDa GST fusion protein. This protein, corresponding to amino acids 769 to 921 within the carboxy-terminal domain of mouse pRb, was obtained from Santa Cruz Biotechnology. This region of pRb includes phosphorylation sites for cyclin E/Cdk2, cyclin D1/Cdk4, cyclin D1/Cdk6 and cyclin A/Cdk2 (22,23). We used this portion of pRb as a substrate to determine cyclin E kinase activity. Tissue lysates were adjusted to equivalent protein levels (500 μg), and pre-cleared with protein-A Sepharose CL-4B (Santa Cruz Biotechnology, Tokyo, Japan) at 4 °C. Samples were incubated with 3 μl (3 μg) of cyclin E polyclonal antibody, or non-immune rabbit IgG used as a control for 4 h at 4 °C. Samples were then immunoprecipitated with 50 μl of 50% (vol/vol) protein-A

Table IV. $p33^{ING1}$ expression and clinicopathologic factors in HCC (logistic regression model)

	No. of patients	$p33^{ING1}$ Expression			Univariate analysis		
		Positive (N,C)	Negative	Negative rate (%)	Odds ratio	95%CI	*P* value
Gender							
Male	61	24 (N:18, C:6)	37	60.7	1.0		
Female	25	15 (N:11, C:4)	10	40.0	0.43	0.17–1.11	0.084
Age (years)							
<65	38	21 (N:18, C:3)	17	44.7	1.0		
	48	18 (N:11, C:7)	30	62.5	1.88	0.79–4.45	0.15
Viral infection							
HCV-positive	77	35 (N:27, C:8)	42	54.5	1.0		
HBs Ag-positive	9	4 (N:2, C;2)	5	55.6	1.04	0.26–4.17	0.954
Histological grade[a]							
WD	17	14 (N:13, C:1)	3	17.6	1.0		
MD&PD	69	25 (N:16, C:9)	44	63.8	8.2	2.15–31.3	0.0021
TNM stage[b]							
I–II	33	21 (N:17, C:4)	12	36.4	1.0		
III–IV	53	18 (N:12, C:6)	35	66.1	3.4	1.37–8.47	0.0083

[a] Histological grading of HCC followed the criteria of the International Working Party.
[b] TNM classification followed that proposed by the Internal Union Against Cancer and American Joint Committee on cancer.
Abbreviations: HCC = hepatocellular carcinoma; HCV = hepatitis C virus; HBs Ag = hepatitis B surface antigen; WD = well-differentiated; MD = moderately differentiated; PD = poorly differentiated; N = nuclear staining; C = cytoplasmic staining; CI = confidence interval; NS = not significant.

Sepharose CL-4B. Immunoprecipitates were washed four times with an immunoprecipitation buffer (50 mM HEPES (pH 8.0), 150 mM NaCl, 2.5 mM ethylene glycol-bis (ß-aminoethyl ether)-N,N,N′,N′-tetraacetic acid, 1 mM EDTA, 1 mM dithiothreitol and 0.1% Tween-20) containing 10% glycerol, 0.1 mM PMSF, 20 U/ml aprotinin, 10 mM ß-glycerophosphate, 1 mM NaF and 0.1 mM sodium orthovanadate. The samples were then washed once with 50 mM HEPES (pH 8.0) containing 1 mM dithiothreitol. Immunoprecipitated proteins on the beads were suspended in 20 μl of kinase buffer (50 mM HEPES (pH 8.0), 10 mM $MgCl_2$, 1 mM dithiothreitol, 2 mM reduced glutathione, 10 mM ß-glycerophosphate, 1 mM NaF, 0.1 mM sodium orthovanadate and 20mM ATP) and then incubated at 30 °C for 30 min with 2 μg of pRb and 10 mCi of [γ-^{32}P]ATP (Daiichikagaku, Tokyo, Japan). After incubation, phosphoproteins were resolved by sodium dodecyl sulphate (SDS) polyacrylamide gel electrophoresis (PAGE; 12.5%) according to the method of Laemmli (24). Phosphorylated GST-Rb fusion protein was visualized by autoradiography or image analysis using a BAS 2000 system (Fuji Film, Tokyo, Japan). Cyclin E kinase activity in each sample was calculated as the mean of three independent measurements.

Gel electrophoresis and Western blot

SDS-PAGE was performed according to Laemmli's method (24), and Western blot was performed as described by Towbin et al. (25), using optimal dilutions of primary antibodies and horseradish peroxidase-linked secondary antibodies. Immunoreactive proteins were visualized with an enhanced chemiluminesescence (ECL) detection system (Amersham, Tokyo, Japan) on X-ray film. Exposures were made for 30 s at room temperature for all samples.

Analysis of cyclin E kinase activity

The phosphorylated band of Rb fusion protein obtained by autoradiography was quantified by image analysis using a BAS 2000 system. The cyclin E kinase activity ratio in a HCC tumour was expressed as a ratio of the tumour's kinase activity to that in normal liver as a control.

Statistical analysis

Data in Tables I and II are expressed as means ± *s* (SD). Factors considered to possibly influence $p33^{ING1}$ expression in HCC included five variables: age, gender, HBs Ag positivity, HCV-RNA positivity, histological grade and TNM stage. Parameters that proved significant in a univariate analysis (Table IV) were then tested using a multivariate logistic regression model (Table V) for 86 patients with HCC. The relationship between five variable factors and $p33^{ING1}$ expression in 86 HCCs was examined using a univariate analysis. In 29 patients, Spearman correlation coefficients were used to evaluate whether $p33^{ING1}$ expression in HCC correlated with relative cyclin E kinase activity and to examine correlations between $p33^{ING1}$ expression, histological grade or TNM stage. The significance of differences between observations presented in Fig. 3C was determined by Student's *t* test. Differences or relationships were considered significant when the associated *P* value was less than 0.05.

Results

Immunostaining for $p33^{ING1}$ in normal liver, chronic hepatitis and liver cirrhosis

The clinicopathological characteristics in the cases of chronic hepatitis and liver cirrhosis are summarized in Table II. Representative immunostaining of $p33^{ING1}$ in cases of

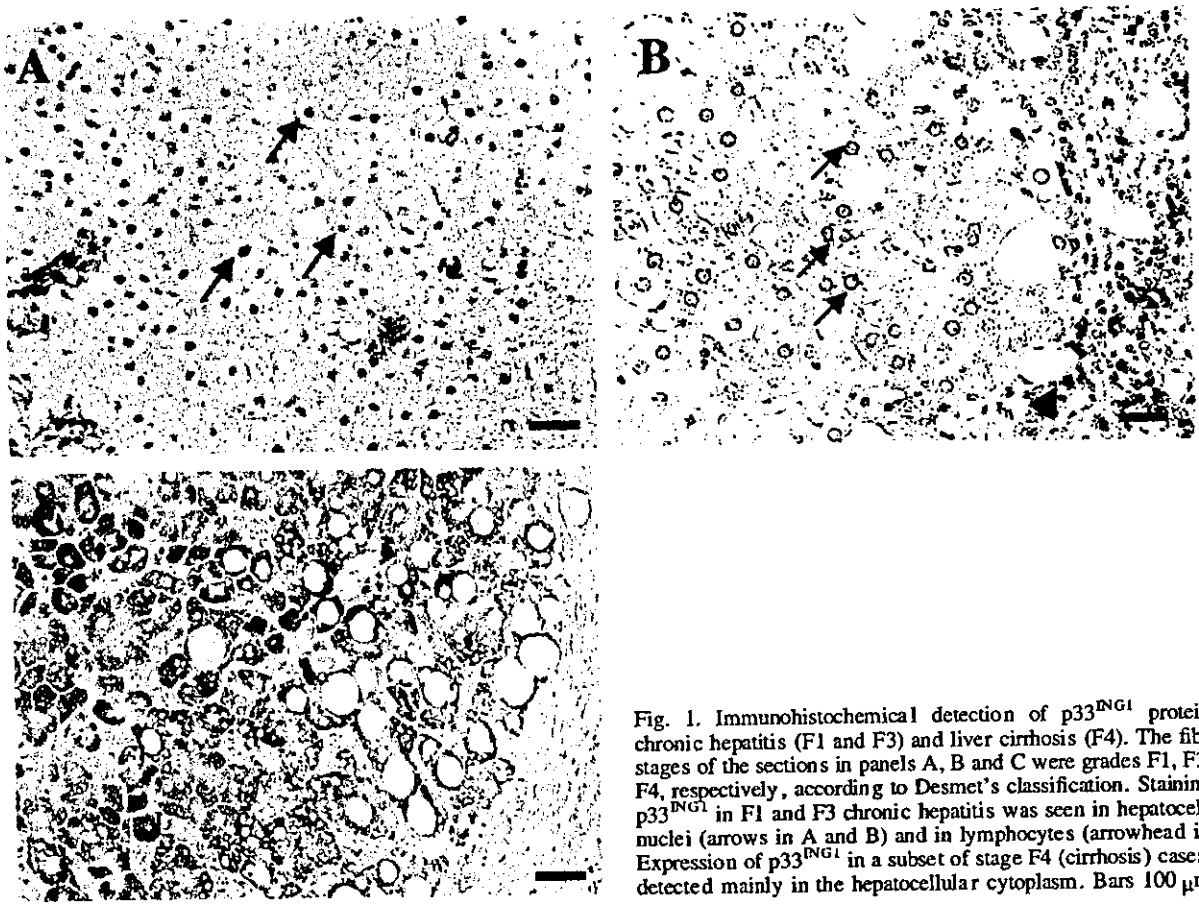

Fig. 1. Immunohistochemical detection of $p33^{ING1}$ protein in chronic hepatitis (F1 and F3) and liver cirrhosis (F4). The fibrosis stages of the sections in panels A, B and C were grades F1, F3 and F4, respectively, according to Desmet's classification. Staining for $p33^{ING1}$ in F1 and F3 chronic hepatitis was seen in hepatocellular nuclei (arrows in A and B) and in lymphocytes (arrowhead in B). Expression of $p33^{ING1}$ in a subset of stage F4 (cirrhosis) cases was detected mainly in the hepatocellular cytoplasm. Bars 100 μm.

chronic hepatitis and liver cirrhosis is shown in Fig. 1. The localization of $p33^{ING1}$ in the F1 (Fig. 1A) and F3 (Fig. 1B) stages of fibrosis was nuclear in hepatocytes (arrows); positive staining was also present in non-pararenchymal cells, including lymphocytes (Fig. 1B, arrowhead). In hepatocytes, immunostaining of $p33^{ING1}$ protein was detected in all 27 chronic hepatitis cases at the F1, F2 and F3 stages in a nuclei distribution. In liver cirrhosis (F4), $p33^{ING1}$ staining was detected in hepatocellular nuclei (Fig. 1C) in 8 of 12 cases (66.7%) and in the cytoplasm of hepatocytes in the remaining cases. In all 5 normal liver specimens, immunostaining for $p33^{ING1}$ was seen in the nuclei of hepatocytes (data not shown).

Immunostaining for $p33^{ING1}$ in HCC

As indicated in Table IV, loss of $p33^{ING1}$ protein was noted immunohistochemically in 47 of 86 patients with HCC (55%). $P33^{ING1}$ expression in the remaining 39 HCCs was detected predominantly nuclear in 29 tumours and predominantly cytoplasmic in 10. When tumours were grouped according to histological differentiation, 14 of 17 well-differentiated HCCs were stained for $p33^{ING1}$ (nuclear in 13, Fig. 2A and B; cytoplasmic in 1, not shown). Among 59 moderately differentiated HCCs, staining for $p33^{ING1}$ was present in 25 (nuclear in 16, cytoplasmic in 9; not shown) but negative in 34 (58%; Fig. 2C and D). In 10 poorly differentiated HCCs, no positive staining for $p33^{ING1}$ was evident (Fig. 2E and F).

Correlations between $p33^{ING1}$ expression and clinicopathological variables, as determined by univariate analysis, are summarized in Table IV. Loss of $p33^{ING1}$ expression was significantly associated with poor histological differentiation and advanced TNM stage. However, no significant relationship was seen between $p33^{ING1}$ expression and gender, age, infection with hepatitis B or C virus, or serum α-fetoprotein concentrations. As some factors might be interrelated, we then performed multivariate analysis (Table V), and found that histological grade and TNM stage were independent determinants of $p33^{ING1}$ protein.

Relationship between cyclin E kinase and $p33^{ING1}$ expression in HCC

To examine whether $p33^{ING1}$ plays a role in controlling cell proliferation through inhibition of cyclin E kinase activity, we studied cyclin E kinase activity in 29 HCC cases, including 5 well differentiated, 19 moderately differentiated and 5 poorly differentiated tumours. Clinicopathological data for these 29 patients with HCC are given in Table III. GST-Rb fusion protein was used as a substrate to measure cyclin E kinase activity. As shown in Fig. 3A, staining of the GST-Rb fusion protein after separation by SDS-PAGE showed a single band

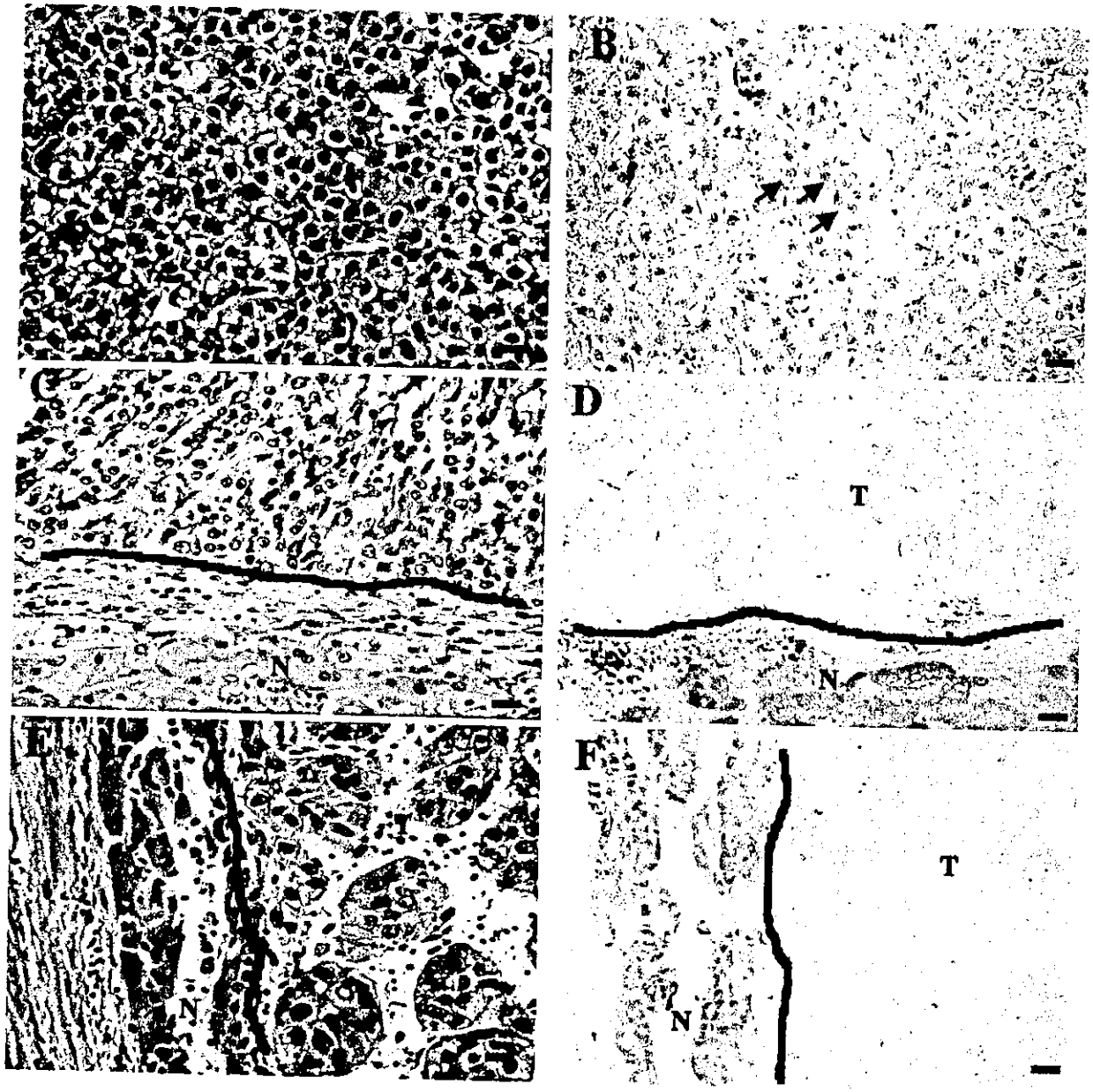

Fig. 2. Localization of $p33^{ING1}$ (B, D and F) in hepatocellular carcinoma (HCC). A and B, well differentiated; C and D, moderately differentiated; E and F, poorly differentiated HCCs. Sections shown in A, C and E were adjacent to those shown in B, D and F, respectively. 'T' and 'N' indicate HCC and non-neoplastic cirrhotic tissues, respectively. Expression of $p33^{ING1}$ in most well-differentiated HCCs was localized to the nuclei of cancer cells (B, arrows), while no staining was seen in most moderately and poorly differentiated HCC, and $p33^{ING1}$ was stained in the cytoplasm of hepatocytes in adjacent non-tumorous cirrhotic tissues (D and F). A, C and E haematoxylin and eosin staining. Bars 100 μm.

with a molecular size of 46 kDa. We confirmed that this band included part of the Rb protein by Western blotting using Rb-specific monoclonal antibody (data not shown). Cyclin E kinase activity was measured by an in vitro kinase assay using the GST Rb fusion protein as a substrate (Fig. 3B). A single band of phosphorylated Rb protein resulting from markedly increased cyclin E kinase activity was detected in all HCC studied. In addition, phosphorylated Rb was not observed in the immunoprecipitation product when non-immune rabbit IgG was used as a control (Fig. 3B). Cyclin E kinase activity was inversely related to the amount of $p33^{ING1}$ expression, although the results must be considered approximate because of the heterogeneous nature of the tumour samples. To summarize, cyclin E kinase activity in $p33^{ING1}$-negative HCC and $p33^{ING1}$-positive HCC (whether staining was cytoplasmic or nuclear) was 18.2 ± 11.8 and 4.8 ± 1.4 times higher, respectively, than that in control normal liver (Fig. 3C). Cyclin E kinase activity in $p33^{ING1}$-negative HCC was significantly higher than in $p33^{ING1}$-positive HCC ($P < 0.001$). In addition, among $p33^{ING1}$-positive HCC,